TOPICAL REVIEW

Reverse Monte Carlo modelling

INSTITUTE OF PHYSICS PUBLISHING JOURNAL OF PHYSICS: CONDENSED MATTER

J. Phys.: Condens. Matter **13** (2001) R877–R913 PII: S0953-8984(01)17949-X

TOPICAL REVIEW

Reverse Monte Carlo modelling

R L McGreevy

Studsvik Neutron Research Laboratory, Uppsala University, S-611 82 Nyköping, Sweden

Received 3 August 2001
Published 2 November 2001
Online at stacks.iop.org/JPhysCM/13/R877

Abstract

Reverse Monte Carlo (RMC) modelling is a general method of structural modelling based on experimental data. RMC modelling can be applied to many different sorts of data, simultaneously if wished. Powder and single-crystal neutron diffraction (including isotopic substitution), x-ray diffraction (including anomalous scattering) and electron diffraction, extended x-ray absorption fine structure and nuclear magnetic resonance (magic angle spinning and second moment) have already been used to provide data. RMC modelling can also be applied to many different types of system—liquids, glasses, polymers, crystals and magnetic materials. This article outlines the RMC method and discusses some of the common misconceptions about it. It is stressed that RMC models are neither unique nor 'correct'. However, they are often useful for aiding our understanding either of the structure itself, or of the relationships between local structure and other physical properties. Examples are given and the possibilities for further development of the RMC method are discussed.

(Some figures in this article are in colour only in the electronic version)

1. Introduction

The physical properties of materials are determined by their atomic structure, so the measurement of experimental data related to the structure, and the production of structural models based on this information, are fundamental to condensed matter science. For most of the twentieth century the emphasis was on crystalline materials, and numerous methods were developed for producing or refining models of the (time-average) structure of crystals based on experimental data. However, non-crystalline materials are of equal, if not greater, technological importance (e.g. liquids, glasses, polymers), yet our structural understanding of these is still relatively primitive and few methods of structural modelling have been developed.

Reverse Monte Carlo (RMC) modelling is a general method of structural modelling based on experimental data [1]. RMC modelling was originally developed for application to the structures of liquids and glasses but has now also been applied to crystalline and magnetic structures [2–5]. Many different sorts of data can be used and many different types of system

can be modelled [6–13]. There are over 400 papers published using RMC methods, yet it is still not unusual to hear comments such as 'It doesn't work' or 'I don't believe it'. Such reactions are due to some common misconceptions. RMC modelling is a method of structural modelling. Its aim is to produce a model, or a series of models, that is consistent with the available data and with any other information supplied in the form of constraints. It is not sensible to ask 'Is the model correct?', since this can in any case never be known. Instead one should ask 'Is the model useful?'. Can it, for example, aid in our understanding of the relationship between the structure and some particular physical property, or help us to suggest further experiments?

This paper reviews the RMC method and its applications. Since the algorithm has been described in detail elsewhere [3, 5, 6, 9–13] it is only outlined briefly, but with sufficient information for those unfamiliar with the method to follow the rest of the paper. Some of the common misconceptions and criticisms are discussed in detail, though they are often philosophical rather than scientific.

Even if RMC modelling is criticized, its greatest success has undoubtedly been to demonstrate that three-dimensional structural models of disordered materials can indeed be produced on the basis of experimental data. This has stimulated the development of derivative and related methods, sometimes with the aim of 'correcting' particular aspects of RMC modelling, and these are discussed. It has also been realized that RMC modelling is not competitive with methods of computer simulation, such as Monte Carlo or molecular dynamics. Rather it is complementary. RMC modelling emphasizes the importance of any form of three-dimensional modelling, but also the importance of details of the experimental data in understanding real (rather than model) materials.

While other methods may provide 'better results' in particular cases, the main strength of RMC modelling is its generality. Examples are given of the application of RMC modelling to a wide variety of types of structure, showing clearly that it is indeed a useful aid to understanding. Finally the prospects for further development are discussed.

2. The RMC method

2.1. The basic RMC algorithm

RMC modelling is a variation of the standard Metropolis Monte Carlo (MMC) method [14]. The aim is to produce a structural model (i.e. an ensemble of atoms, usually referred to as a configuration) which is consistent with one or more sets of experimental data within their errors and subject to a set of constraints. The errors are assumed to be purely statistical and to have a normal distribution (this will be discussed in more detail later). The method is outlined here for application to neutron diffraction data for a liquid or glass. The extension to different data types has been described elsewhere (e.g. [5]). The most widely used program which implements this algorithm is known as RMCA [9].

(1) N atoms are a placed in a cell with periodic boundary conditions, i.e. the cell is surrounded by images of itself. Normally cubic cells are used but other geometries may be chosen, e.g. to make a supercell of a crystalline unit cell. The cell dimensions should be as equal as possible. The atomic number density should be the same as the experimental value. The positions of the atoms may be chosen randomly; they may have a known crystal structure or they may be taken from a different simulation or model. The combination of atom coordinates and cell geometry/dimensions is known as a configuration.

(2) Calculate (C) the partial radial distribution functions (also known as the pair distribution functions) from the configuration:

$$g_{\alpha\beta}^{Co}(r) = \frac{n_{\alpha\beta}^{Co}(r)}{4\pi r^2 \, \mathrm{d}r \; \rho c_\alpha} \tag{1}$$

ρ is the atomic number density, c_α is the concentration of atoms type α and $n_{\alpha\beta}^{Co}(r)$ is the number of atoms type β at a distance between r and $r + \mathrm{d}r$ from a central atom of type α, averaged over all atoms as centres. Superscript o means 'old' and its significance will become clear in the following steps.

(3) Fourier transform $g_{\alpha\beta}^{Co}(r)$ to obtain the partial structure factors:

$$A_{\alpha\beta}^{Co}(Q) = \rho \int_0^\infty 4\pi r^2 (g_{\alpha\beta}^{Co}(r) - 1) \frac{\sin Qr}{Qr} \, \mathrm{d}r \tag{2}$$

where Q is the momentum transfer.

(4) Calculate the total structure factor

$$F^{Co}(Q) = \sum c_\alpha c_\beta b_\alpha b_\beta (A_{\alpha\beta}^{Co}(Q) - 1) \tag{3}$$

where b_α is the coherent neutron scattering length for atom type α.

(5) Calculate the difference between the measured total structure factor, $F^E(Q)$, and that determined from the configuration, $F^{Co}(Q)$:

$$\chi_o^2 = \sum_{i=1}^{m} (F^{Co}(Q_i) - F^E(Q_i))^2 / \sigma^2(Q_i) \tag{4}$$

where the sum is over the m experimental points and σ nominally represents the experimental error. Note that the minimum Q_i-value used should be larger than or equal to $2\pi/L$, where L is the minimum dimension of the configuration.

(6) Move one atom at random; in practice there is a maximum move distance. If any two atoms approach closer than a predefined (cut-off) distance, then the move is rejected, a new atom is chosen and a new move is made.

(7) Calculate the new partial radial distribution function, $g_{\alpha\beta}^{Cn}(r)$, the new partial structure factors, $A_{\alpha\beta}^{Cn}(Q)$, the new total structure factor $F^{Cn}(Q)$, and the difference

$$\chi_n^2 = \sum_{i=1}^{m} (F^{Cn}(Q_i) - F^E(Q_i))^2 / \sigma^2(Q_i). \tag{5}$$

(8) If $\chi_n^2 < \chi_o^2$, then the move is accepted, i.e. the 'new' configuration becomes the 'old' configuration. If $\chi_n^2 > \chi_o^2$ it is accepted with probability $\exp(-(\chi_n^2 - \chi_o^2)/2)$. Otherwise it is rejected.

(9) Repeat from step 6.

As the number of accepted atom moves increases, χ^2 will initially decrease until it reaches an equilibrium value, about which it will then oscillate. The resulting configuration should be a three-dimensional structure that is consistent with the experimental data within its errors. Here we have chosen to fit the structure factor, although a radial distribution function determined from the experimental data could also be fitted. Figure 1 shows an example of RMC modelling of a simple test system.

In MMC modelling the quantity sampled is $(U_n^2 - U_o^2)/kT$ where U is the potential energy of the configuration based on a given interatomic potential, T is the temperature and k is Boltzmann's constant. The structure factor therefore plays the role of the energy, i.e. it 'drives' the model, and σ plays the role of the temperature. The exact definition of χ^2 is

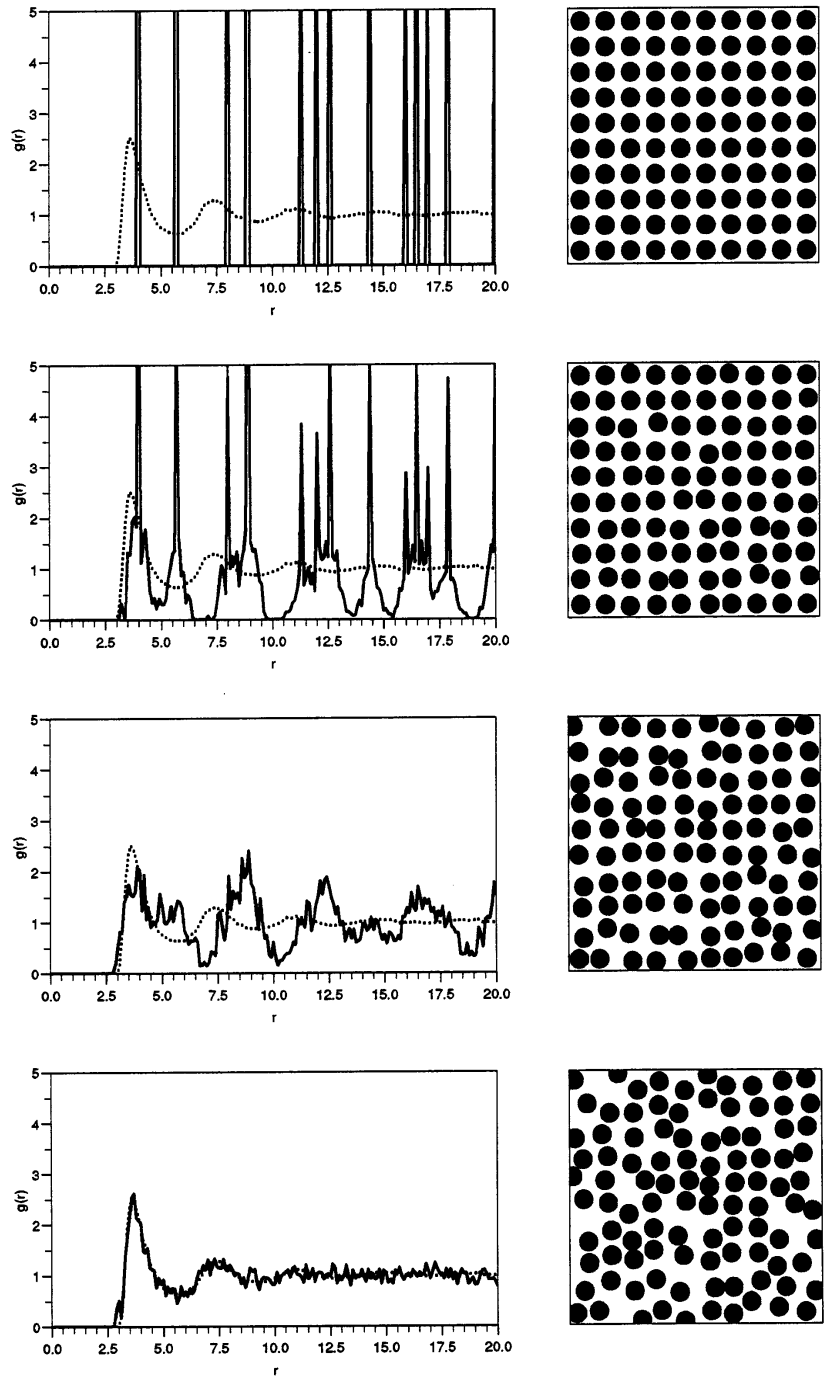

Figure 1. An example of RMC modelling of a simple test system. The configuration (two-dimensional) is shown on the right and on the left $g^C(r)$ (solid curve) is compared to the target data, $g^E(r)$ (broken curve), obtained by Metropolis Monte Carlo simulation using a Lennard-Jones potential. The starting configuration is at the top, the final configuration at the bottom and two intermediate configurations in between. In this example a total of 2500 accepted moves were made. Note that $g^C(r)$ is statistically noisy due to the small model size.

not particularly important. The aim of MMC modelling is to produce a configuration with a Boltzmann distribution of energies, but the aim of RMC modelling is simply to produce a model which is consistent with the data within its errors, of which systematic errors (with an unknown distribution) are usually the most important. The form of χ^2 is chosen because the analogy with MMC modelling is convenient, and because it works!

There are several key features of the RMC algorithm, which made it generally successful compared to earlier attempts or related methods (e.g. [15–18]).

(1) Periodic boundary conditions are used to avoid edge effects, and in practice models are large (at least several thousand atoms) to avoid finite-size effects.
(2) Some moves that increase χ^2 are accepted, so the result can be (in principle) independent of the initial configuration.
(3) If possible the experimental data are fitted (e.g. the total structure factor), as opposed to function(s) derived from the data (e.g. the partial radial distribution functions), or a set of parameters derived from the data (e.g. short-range-order parameters [17, 18]). This makes it much easier to understand the effects of errors. For example, if three total structure factors measured by means of neutron diffraction with isotopic substitution are available and one contains significant errors, then this will be obvious immediately, whereas if three partial radial distribution functions derived from the data are fitted, then all will contain significant errors.
(4) No interatomic potential is used in the conventional sense, though the atomic closest-approach constraint can be thought of as a hard-sphere potential. RMC modelling can therefore be applied to any system. Other aspects of the use of potentials are discussed later. The lack of a potential has the disadvantage that RMC models have no thermodynamic consistency. However, use of a potential can imply some contradictions. If the potential is fixed and is not compatible with the data, then either χ^2 can be minimized, or the energy, but not both. If the potential is modified to fit the data, then the form of the potential must be appropriate. If a wrong form is chosen (e.g. a two-body potential when many-body forces are significant), then this may bias the fitting towards a wrong result. The use of potentials is discussed further in section 5.3.

The RMC algorithm is easily modified for simultaneous fitting to different sets of data, as long as the function representing the data (e.g. $F(Q)$) can be calculated in terms of the configuration. For each data set a separate χ^2 is defined and these are simply summed. Data sets are weighted relative to each other by the use of different σ-values. The types of data which have been used are from neutron diffraction (including isotopic substitution (e.g. [19])), x-ray diffraction (including anomalous scattering (e.g. [20])), electron diffraction [8], extended x-ray absorption fine structure (EXAFS (e.g. [21])) and NMR (magic angle spinning [22] and second moment [23]). The largest number of data sets that have been simultaneously fitted so far is five, from four different experimental techniques [23, 24]. In practice the limitation is the experimental difficulty of collecting consistent multiple data sets, rather than the RMC method. A particular advantage of RMC modelling is that data sets can be measured over different ranges and with different resolutions and can even contain 'holes'; e.g. known 'bad' data points can be removed. However, clearly RMC modelling cannot replace missing information.

2.2. *Constraints*

Another key feature of the RMC method is the use of constraints. The most important are the density and the use of closest approaches (cut-offs); these are a necessary part of the basic algorithm. The initial factor determining any structure is packing, so it makes sense to include

it from the start. Without these constraints, RMC modelling would be able to fit any data set, however large the errors, as long as the number of data points was less than the number of variables in the modelling (i.e. $3N$). However, with the constraints, the atomic coordinates are no longer free variables; instead they are highly constrained. This is easily demonstrated by the fact that RMC modelling cannot fit many data sets, since they contain significant systematic errors. Indeed the application of density and closest-approach constraints allows simple systematic errors, such as incorrect normalization or a constant background, to be corrected for automatically during RMC modelling.

The choice of cut-offs is not always obvious and can be important if insufficient data are available. Since there must be at least one data set, the shortest cut-off can always be estimated from direct determination of the radial distribution function. In the absence of any other information this should also be used as the cut-off distance for all atom pairs. If several data sets are available, then it may be possible to estimate cut-offs for several atom pairs. In most cases it is also possible to make estimates using other information, for example atomic or ionic radii and results for related systems. In the absence of detailed information, cut-offs should always be underestimated, since otherwise this biases the resulting structure and can lead to poor fitting of the data.

The next most commonly used constraint is on atomic coordination. In a sense this acts to mimic covalent bonding and hence could be thought of as a form of many-body potential. It can be applied in a number of ways, either as a 'hard' or 'soft' constraint. A coordination number is defined as the number of atoms of type β within two fixed distances of one of type α. Normally the lower fixed distance is the closest approach of atoms α and β. If we define the fraction of atoms of type α in the configuration which satisfy the coordination constraint as f_{RMC}, and the required fraction as f_{req}, then a term

$$\chi^2_{coord} = (f_{req} - f_{RMC})^2/\sigma^2_{coord} \tag{6}$$

is added to the overall χ^2. σ_{coord} is used to weight the coordination constraint relative to the data. If it has a very small value (effectively zero), then the constraint is 'hard', so once an atom has attained the required coordination it cannot lose it. A larger value of σ_{coord}, i.e. a soft constraint, will act to increase the probability of the chosen coordination. Clearly multiple constraints may be applied just by adding more χ^2-terms. Atom types may be mixed. For example in vitreous silica one may constrain all Si to be coordinated to four O and all O to two Si, while in hydrogenated amorphous Si one may constrain all H to be coordinated to one Si and all Si to be fourfold coordinated but to any combination of Si and H.

The average atomic coordination can also be constrained. This is rarely used, but might be appropriate if for example a set of EXAFS data could be used to give an approximate value for an average coordination number, but for some reason the data themselves could not be modelled directly.

Another method is to constrain the coordination of individual atoms, rather than atom types, e.g. atom 247 in the configuration is coordinated to atom 591 [25]. This is a hard constraint and is applied by providing a list of constrained atom pairs and distances. For example, in liquid CS_2 the intermolecular and intramolecular C–S distances overlap so an atom type constraint does not work. However, if each individual C atom is constrained to be coordinated to two individual S atoms, then individual CS_2 molecules are maintained regardless of the positions of other molecules. Rather complex units such as polymers can be maintained in the same way.

In principle constraints of any required complexity can be applied. Those described so far apply to pairs of atoms. Three-atom constraints, such as on bond angles, can also be applied [26, 27]. However, it should be noted that these are considerably more computationally

expensive. In the same way, application of too many hard constraints, as might be required to describe large rigid molecules, can become too expensive to be practical.

2.3. *Consistency of data and constraints*

All experimental data contain errors, which are commonly underestimated. This means that, even if a constraint is 'known' to be correct, it might not be consistent with a particular data set. Similarly different data sets might not be consistent with each other. In such cases an RMC model cannot be expected to fit all of the data and constraints—this may be a fault of the model (it may be stuck in a 'local minimum'), but more frequently it is the fault of the data or constraints. For example, relatively rigid covalent bonds give rise to high-Q oscillations in a neutron diffraction pattern. However, inelastic scattering effects can broaden and de-phase these oscillations in a way that we do not yet know how to correct for. This can result either in a coordination number from the data that differs from the 'correct' value, or an effective broadening of the allowed bond lengths compared to those obtained from e.g. spectroscopy. If the RMC model is constrained to the 'correct' coordination or a narrow bond-length distribution, then it will not fit the data as well. It must be left to the judgment of the user whether the constraint or data is given greater weighting. For example, it is normally considered that the Si–O coordination in vitreous silica is fourfold. However, an excellent fit to neutron and x-ray diffraction data, as shown in figure 2, is only achieved with a coordination of 3.75 [28].

It has already been noted that the imposition of fixed density and closest-approach constraints in RMC modelling allows automatic correction for flat background and normalization errors in the experimental data. Another typical systematic error is a low-order-polynomial background, and while RMC modelling cannot correct for this it is also normally not possible to fit it, since it would imply atoms at unphysically close distances. If the difference between RMC fit and data has this form, then it is usually a reliable indication of an error in the data. If the error is uncorrelated with the form of the data, then an approximate correction can be made by simply subtracting a polynomial fitted to the difference (this is also possible using the MCGR program [29]). However, if the error is correlated with the form of the data, such as in the case of magnetic scattering that has been ignored, then the data-fit difference may not be a good representation of the error and should not be used as a correction.

These features make RMC modelling a valuable tool for data quality control. Even if a user only produces the simplest atomic model, and never even looks at it, the comparison of data and RMC fit can provide very rapid feedback on the individual quality and consistency of different data sets.

2.4. *Creating initial configurations*

Although the result of RMC modelling is in principle independent of the starting configuration, subject to the constraints applied, in practice this condition takes too long to achieve except for the simplest liquids. The creation of initial configurations is therefore a key step, and so some comments on different methods should be made here. We will restrict ourselves to those methods closely associated with RMC software and methodology. A common approach is to use the RMCA program but without fitting to any data. This is then equivalent to a hard-sphere Monte Carlo simulation (HSMC, or CSHMC if coordination constraints are applied).

When modelling non-molecular liquids, the simplest approach is to create a random configuration of points and then run HSMC to equilibrium with appropriate cut-offs. For molecular liquids the molecules must be 'predefined' since the later application of coordination

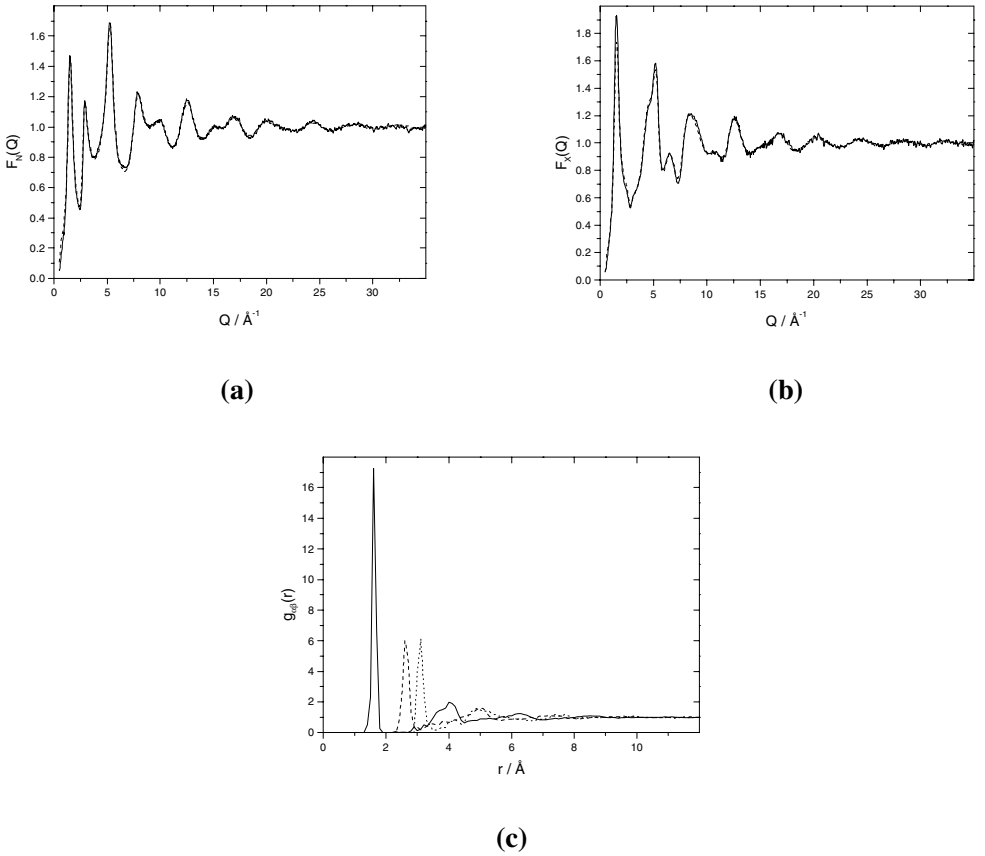

Figure 2. Experimental structure factors (solid curves) for vitreous SiO_2 derived from (a) neutron diffraction and (b) x-ray diffraction compared to RMC fits (dashed curve). (c) $g_{\mathrm{SiO}}(r)$ (solid curve), $g_{\mathrm{OO}}(r)$ (dashed curve) and $g_{\mathrm{SiSi}}(r)$ (dotted curve) from the RMC model [28].

constraints may produce a high proportion of molecules, but it will not be 100%. If a configuration of molecules with random positions and orientations is created, then there will initially be some intermolecular distances that are too short. Individual atom coordination constraints within CHSMC can be used to maintain the bonding while satisfying the required cut-offs. Atom type coordination constraints should not be used.

Polymers are rather complex molecular liquids and here different methods are required. Random-walk procedures that build chains monomer by monomer, back-tracking when monomers overlap, work well for simple monomers but can rapidly become stuck for long chains of monomers with bulky side groups. Potential-based methods are possible where single straight chains are made and then relaxed—however, these methods can prevent certain chain topologies which can occur in reality. For RMC modelling a hybrid method has been developed [30], which can be illustrated for the case of polypropylene oxide [31]:

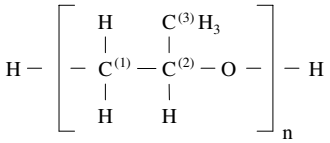

(1) The initial backbone chain, $(–C^{(1)}–C^{(2)}–O–)_n$, is created by a standard random-walk procedure, with the configuration dimensions determined from the required density for the complete polymer. Since there is plenty of free volume, this is a simple procedure. The chain ends are terminated appropriately.
(2) The next step is to place two H atoms unphysically close to carbon $C^{(1)}$ and one carbon $C^{(3)}$ and one H atom close to $C^{(2)}$. CHSMC is run, using appropriate constraints to maintain the bonding, until the required cut-offs are satisfied.
(3) Three H atoms are similarly added close to $C^{(3)}$ to produce a CH_3 group, and CHSMC is again run.

This type of procedure is relatively slow but it can be used to produce polymers of any complexity.

For modelling liquids it is not advisable to start from a crystal structure, even at the correct density for the liquid, since there is still usually not enough free volume for the crystal to 'melt' completely. The result will be a highly disordered crystal, not a liquid, though this may not be obvious from the calculated structure factor or even from looking at the configuration. However, for modelling crystals it is clearly advisable to start from the average crystal structure, as determined by one of the conventional crystallographic methods. Wherever possible the lattice parameters should be obtained from the same data that are to be fitted with RMC modelling, to ensure consistency.

The most complex systems for which to produce initial configurations are network glasses. The use of coordination constraints means that the complete network topology remains fixed during fitting, so RMC modelling is restricted to relatively limited refinement of the initial coordinates. Nevertheless the method has been surprisingly successful, which indicates that in many cases the bonding topology, largely determined by the chemistry, is the key to the structure. For $(K_2O)_x(SiO_2)_{1-x}$ glasses the following procedure was used [22].

(1) A random configuration of Si atoms is created, at a density corresponding to that in the final glass.
(2) CHSMC is run with coordination constraints on Si neighbours. Numbers for twofold, threefold and fourfold coordination correspond to the numbers of Si with two, three or four bridging oxygens required in the final model, these numbers being determined from magic angle spinning NMR data. The Si–Si distances are set to be less than twice the allowed range of Si–O distances in the final model. A constraint can also be applied to prevent the formation of three-membered rings if required [22].
(3) When the coordination constraints are satisfied, O atoms are added at all Si–Si bond centres. These are the bridging oxygens.
(4) O atoms are added near to Si atoms which have fewer than four O neighbours. These are the non-bridging oxygens.
(5) CHSMC is run with a constraint of fourfold Si–O coordination and twofold O–Si coordination until all closest-approach constraints are satisfied. A constraint on the Si–O–Si bond-angle distribution can also be applied if required [27].
(6) The result is a silicate network with the required topology. K atoms are then added at random.

3. Some common misconceptions

So far we have largely described the technical details of RMC modelling. However, it is important to also take a more general overview in order to avoid some common misconceptions about the method, and related criticisms. The most usual criticism is that RMC models are not

unique, which leads illogically to the statement that they are therefore not correct and hence the method is not useful. Several points must be made here.

- One can never know the 'true' structure of any material, in the sense that one knows the exact positions of all the atoms, or even of any subset of the atoms. This applies to both crystalline and non-crystalline materials. For a start the structure is not static. Even in the simplest case, and except at zero temperature, atoms vibrate, so there is a difference between the time-average atomic positions and the positions at an instant in time.
- Experimental data provide incomplete information about correlations between atoms (e.g. diffraction) or projections of some density distribution (e.g. electron microscopy). From this incomplete information scientists normally try to make a model which is a useful description of some aspect of the 'structure'. The fact that this might be called 'solving the structure' rather than 'making a model', does not mean that the 'solution' is either unique or correct. RMC modelling is no different in this context from any other method of structural modelling.
- An RMC model is not unique. This is one of the main advantages of the method—it is not a disadvantage. If a method can only produce a single model, then that model is unique to that method, but that does not mean either that it is 'correct' or that no other model is possible based on the same data.
- RMC modelling allows one to explore, for example by the imposition of different constraints or the use of different initial configurations, a range of structural models that are consistent with the available data. However, because there will always be an infinite set of consistent structural models (regardless of the number, type or quality of the data) the user must make some choice as to how far to go. Different models could be used to make predictions of the results to be obtained by further experiments, which could then be tested. Such an application of RMC modelling is therefore an excellent example of classical scientific methodology!
- This brings us to the key point. RMC modelling is a method of structural modelling—nothing else. However, the atomic coordinates in the model are of themselves of no direct interest. What matters is whether the models are useful. Can they be used to help our understanding of some aspect of the material, for example the relationship between the structure and some physical property?

Some more detailed points can also be made.

- RMC models are statistical. They will always contain, at some level, errors ('structural defects') which can be readily identified but not always so readily removed. Indeed sometimes defects in the model are intrinsic to errors in the data and attempting to remove them will only produce different defects. A small number of defects does not necessarily invalidate the usefulness of a model.
- RMC models are sometimes criticized because they do not show certain features which are 'known' to be correct. This is not the fault of the methodology. RMC models are based on the data and constraints provided. If the missing features do not necessarily follow from the data and constraints provided, then they must be based on additional information that has not been provided. If that information was provided, either in the form of additional data or constraints, then the missing features should 'appear'. The same would apply to features that do appear in the model but are 'known' to be wrong.
- However, it is not unusual to find that 'known' features are only ideas that have been suggested to explain previous data. (As the literature on a subject develops 'X has proposed $\cdots$' becomes 'X has shown $\cdots$' and finally 'It is well known that $\cdots$'.) If an RMC model

independently produces the proposed feature, then this lends strong support to the idea. If it does not, then the feature may still be shown to be consistent with the data by imposition of a suitable constraint. On the other hand, it may be found to be inconsistent. Sometimes even apparently opposing features are found to be consistent with a single model [32]!

- If an RMC model produces features that are 'unexpected', they should not simply be dismissed. Again, an objective approach is more valuable than a subjective reaction. RMC modelling tends to produce the most disordered structure that is consistent with the data and constraints (though in practice this is also dependent on the starting configuration and the exact run parameters chosen). It is therefore unlikely that unexpected order will appear unless driven by the data and constraints, so such features should be considered seriously. Conversely there is a tendency to follow Occam's razor, that if a simple solution to a problem can be found, then it tends to be the correct solution, and hence to dismiss apparently complex solutions. In the case of disordered structures that are driven by entropic forces, for example, this might be a mistake.

Some of the misconceptions arose due to a paper by Evans [33] during the early days of RMC modelling. He showed that for a system which can be described by a pairwise-additive potential (i.e. two-body forces only), there is a unique functional relationship between the pair correlation function and the potential. The potential determines all higher-order correlation functions and hence the 'structure'. This was misinterpreted by some (not by Evans) as suggesting that RMC modelling should produce the 'correct' answer, and if it did not, then the method must be wrong. However, the result is not *directly* relevant to RMC modelling, for four reasons.

- The pair correlation function (or correspondingly the structure factor) must be known exactly and over an infinite range. Real data are neither exact nor infinite.
- We do not know what the functional relationship is, merely that it exists.
- Only a relatively limited number of systems are described adequately by pairwise-additive potentials.
- The theory only states that the exact pair distribution function is required to obtain the pair potential uniquely, and hence all of the higher-order correlation functions. It says nothing about how sensitive any of these functions are to deviations from exactness (this point has recently been made by Soper [34]).

Evans' result is certainly relevant to RMC modelling in an indirect sense, since it suggests that an accurately measured structure factor does contain a great deal of information about both two-body and higher-order correlations, and that the information content increases with the accuracy and range of the data. However, if the many-body contributions to the potential are large, then two-body data are likely to be insufficient, hence the introduction of e.g. coordination constraints in RMC modelling.

There have been several test studies of RMC modelling to investigate the extent to which many-body correlations can be derived from the pair correlation function or structure factor. Howe and McGreevy [35] found that for a monatomic system simple three-body correlations were well reproduced, though the statistical fluctuations in both two- and three-body correlations tended to be suppressed. For a model of diatomic molecules, i.e. one with significant non-pairwise-additive forces, unconstrained RMC modelling does not work. It produces a mixture of atomic coordinations, even if the required (onefold) coordination does dominate. However, if an appropriate coordination constraint is applied, then reasonable results were obtained. Colognesi *et al* [36] also looked at orientational correlations for model diatomic molecules, but came to the conclusion that RMC modelling did not reproduce them

well. However, Soper [34] has performed a series of test studies which show that a variety of two-body potentials can be generated using the EPSR method (see section 5.3), both for atomic and molecular systems, which reproduce the original three-body correlations well. This supports the conclusions of Howe and McGreevy [35].

The different conclusion of the Colognesi *et al* study [36] may be due to the method of 'quality assessment' used. Five specific orientational correlation functions were calculated, but the typical fluctuations were not determined. For example, how much do the functions vary between individual configurations of the original model, or with small variations in the angular limits defining them, i.e. how *significant* are the differences between RMC modelling and the original model when analysed in terms of these functions? Soper [34] used a single general angular correlation representation, illustrated in figure 3. Here the 'quality assessment' is made on a visual basis.

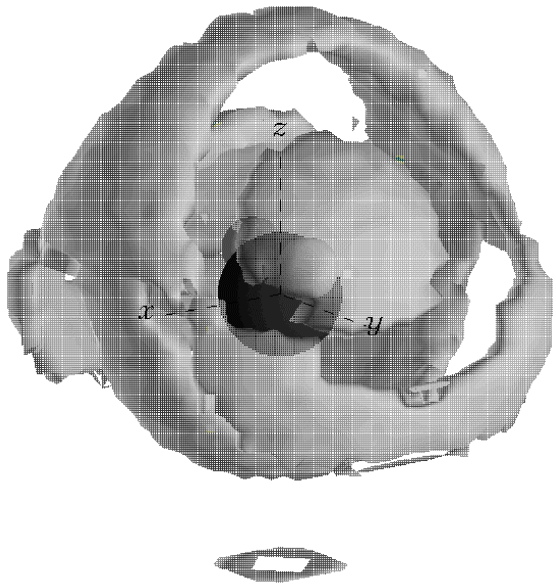

Figure 3. The spatial density function for water derived from EPSR modelling [34]. At the centre of the plot a water molecule is shown with a set of coordinate axes. The density surfaces outside this correspond to the relative density of water molecules as a function of polar coordinates (r, θ, ϕ) within this coordinate system. The isosurface shown corresponds to a density of 1.35 $\times$ the bulk water density.

While this type of test study is interesting, it must still be stressed that the results of modelling 'real' data, whether using RMC modelling or any other method, should always be approached with both caution and an open mind. If specific many-body correlations are of detailed interest, then appropriate constraints should be used to explore the range of such correlations consistent with the data.

4. Variations on the basic RMC method

4.1. Rigid molecules

For relatively rigid molecules it may not be efficient to move individual atoms, so a separate RMC program (RMCMOL) was developed in which the 'moves' consisted of translations and

rotations of predefined groups of atoms, i.e. molecules [37, 38]. However, in practice it was found that this was no more efficient than atom moves. Because of the strong steric constraints, only small moves of molecules were accepted with any high probability. In addition there were some specific disadvantages.

- The molecule must be predefined. The relevant information is usually obtained by fitting to the high-Q part of the structure factor to obtain the intramolecular form factor. The form factor is in fact largest at low Q, but in this region it overlaps with the intermolecular correlations. Any error in fitting the form factor will be magnified at low Q and lead to an error in the intermolecular structure factor which is the function being fitted in RMCMOL. This problem is well illustrated by work on liquid phosphorus where a rigid-molecule approach could not obtain a good fit to the data [39], whereas an atomic model with coordination constraints could [40].
- In calculation of the structure factor the intramolecular motions are taken care of by introducing a Debye–Waller factor into the form factor. However, the actual RMC model only contains rigid molecules. This is an inconsistency since the model now effectively has a larger free volume than is available in reality. This has also been given by Soper [34] as one of the reasons that (Monte Carlo or molecular dynamics) simulations of water using rigid molecules do not agree well with experimental pair distribution functions. Obviously the rigid-molecule approach becomes less applicable as the molecules become more flexible.

4.2. The convolution method for powder crystalline materials

In section 2.1 it has been stated that RMC modelling can be used to fit to the experimental structure factor, $F^E(Q)$, or the radial distribution function, $g^E(r)$. Either $F^C(Q)$ is obtained by Fourier transforming $g^C(r)$, or $g^E(r)$ must be obtained by transforming $F^E(Q)$. In neither case do we want to have errors introduced by truncation of the function being transformed. To obtain $g^E(r)$ this means that we must measure $F^E(Q)$ to a high Q-value, or use an inverse method to obtain $g^E(r)$ (e.g. MCGOFR [41] or MCGR [29]). To obtain $F^C(Q)$ we need to make the RMC configuration large enough that $g^C(r)$ is flat at the highest r-value which can be calculated (half of the cell edge in the case of a cubic cell). For most liquids and glasses this condition is satisfied with models of a few thousand atoms. However, for crystalline materials, which have long-range order, it would require models of billions of atoms. Two approaches can then be used. Either we can model $g^E(r)$, or we can model $F^E(Q)$ but take into account the r-space truncation due to the finite RMC model size [42]. This is done by convoluting $F^E(Q)$ with the Fourier transform of the truncation function:

$$m(r) = \begin{cases} 1 & r < L/2 \\ 0 & r > L/2. \end{cases} \tag{7}$$

Mellergård [43] has pointed out that the equations originally given by Nield *et al* [42] are not strictly correct and that the function to be convoluted is actually $QF^E(Q)$, i.e.

$$F_L^E(Q_j) = \frac{1}{\pi Q_j} \int Q_i F^E(Q_i) \left(\frac{\sin(|Q_i - Q_j|L/2)}{|Q_i - Q_j|} - \frac{\sin(|Q_i + Q_j|L/2)}{|Q_i + Q_j|} \right) \mathrm{d}Q_i. \tag{8}$$

Figure 4 shows an example of convoluted data and a fit for ND_4Cl [44]. The error in the equations explains the fact that the oscillations in the fit at low Q are slightly larger than those in the convoluted data. The figure also shows that the convolution method must still

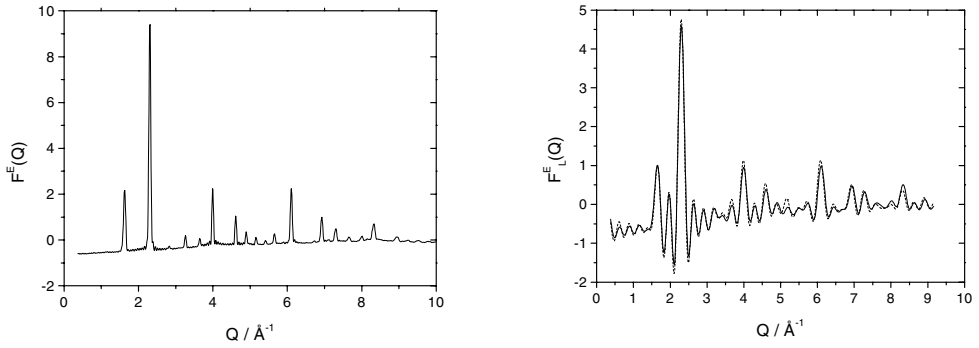

(a) **(b)**

Figure 4. (a) $F^E(Q)$ measured experimentally for ND_4Cl [44]. (b) Convoluted $F^E_L(Q)$ (solid curve) and the RMC fit (dashed curve).

necessarily lose information on long-range order since it introduces an effective Bragg peak broadening—weak peaks tend to 'disappear', particularly when they are close to strong peaks. For this reason a new method was developed for crystalline materials, as described in the next section.

4.3. Direct calculation method for powder crystalline materials

The direct calculation method for powder crystalline materials has been implemented in the RMCPOW program and described in detail elsewhere [12, 13, 45, 46]. The configuration cell is chosen to be a supercell of the crystal unit cell and the total structure factor, $F(Q)$, is calculated using the expression

$$F(\boldsymbol{Q}) = \frac{1}{N}\sum_{j,j'=1}^{N} \langle \mathrm{e}^{-\mathrm{i}\boldsymbol{Q}\cdot(\boldsymbol{R}_j(0)-\boldsymbol{R}_{j'}(0))}\rangle = \frac{1}{N}\left|\sum_{j=1}^{N}\mathrm{e}^{-\mathrm{i}\boldsymbol{Q}\cdot\boldsymbol{R}_j(0)}\right|^2 \tag{9}$$

where the sum is over all N atoms in the sample with positions $\boldsymbol{R}_j(t=0)$, i.e. atoms in the configuration cell. $F(Q)$ represents total (energy-integrated) scattering—that is, both Bragg and diffuse scattering. In conventional crystallography only the elastic Bragg scattering is considered and the elastic structure factor is

$$S(\boldsymbol{Q}) = \frac{1}{N}\sum_{j,j'=1}^{N}\int \langle \mathrm{e}^{-\mathrm{i}\boldsymbol{Q}\cdot\boldsymbol{R}_j(0)}\mathrm{e}^{\mathrm{i}\boldsymbol{Q}\cdot\boldsymbol{R}_{j'}(t)}\rangle \,\mathrm{d}t. \tag{10}$$

To a first approximation (i.e. assuming small harmonic motions) the integral can be performed and the sum over the N atoms in the sample (configuration) replaced by a sum over the N_c atoms in the crystallographic unit cell, giving the more familiar expression

$$S(\boldsymbol{Q}) = \frac{1}{N_c}\mathrm{e}^{-WQ^2}\left|\sum_{k=1}^{N_c}\mathrm{e}^{-\mathrm{i}\boldsymbol{Q}\cdot\langle\boldsymbol{R}_k(t)\rangle}\right|^2. \tag{11}$$

$\langle\boldsymbol{R}_k(t)\rangle$ are the time-average positions of atoms in the unit cell and W is the Debye–Waller factor (DWF) which is related to the mean square deviation (msd) of atoms from their average positions.

$S(Q)$ is therefore determined by the correlations between the time-average atomic positions (equation (11)), while $F(Q)$ is determined by the correlations between the instantaneous positions (equation (9)). More simply put, the elastic structure factor gives us a 'time-average picture' of the structure of the material, while the total structure factor gives us an instantaneous 'snapshot picture'. Both pictures are space averages ($\langle\cdots\rangle$ indicating that functions are averaged over all atoms taken as the origin), but only at $T = 0$ are they the same. At other T the structure is not static but dynamic and so neither picture is 'correct'. Which picture is more useful depends on the problem being investigated. For most crystallographic studies the time-average structure is the subject of interest and so elastic scattering is sufficient. In a liquid, on the other hand, all atoms are diffusing, so there is no time-average structure and hence no strictly elastic scattering—only the instantaneous structure is meaningful. For crystalline structures with dynamical disorder, for example fast-ion conductors, both time-average and instantaneous structures may be of interest.

While it would be possible to make RMC models of the average structure of crystalline materials, based on the elastic structure factor, this has never been done except in simple tests. There are numerous other methods of modelling average crystal structures that are considerably faster. However, it is worth noting that there are Monte Carlo methods for crystal structure solution/refinement that are conceptually very close to RMC modelling (e.g. [47]). On the other hand, RMC modelling is able to model the instantaneous structure based on the total structure factor, and hence provide information on local atomic correlations in crystals, which is not possible with conventional crystallographic techniques.

Because an RMC configuration has periodic boundary conditions, $F(Q)$ as calculated via equation (9) is actually the Bragg scattering of the supercell. This consists of many peaks since the supercell is large; the unit cell peaks are a small subset. If there are no atomic displacements, then all the supercell peaks that are not unit-cell peaks have zero intensity. When there are small atomic displacements, then all of the peaks can have non-zero intensity, but the unit-cell peaks tend to be most intense. As the configuration size increases the additional supercell peaks will merge and form a background—the diffuse scattering. This means that if we can produce an RMC model that is large enough, then a direct calculation of the scattering via equation (9) will give a reasonable approximation to both the Bragg and diffuse scattering. Because the pattern is calculated directly in Q-space it can easily be convoluted with the experimental resolution function.

If the sample is magnetic, then a simultaneous model of the magnetic structure can be made, with the magnetic scattering being calculated according to similar principles [13]. In practice for an RMC model of reasonable size, say 4000 atoms, the supercell peaks are sufficiently numerous but are not uniformly distributed in Q. At low Q, where the peaks are sparse, it is necessary to smooth between them to obtain a good estimate of the diffuse scattering [13, 46]. A particular advantage of RMCPOW is that the results for the average structure can be compared directly to Rietveld refinement of the elastic structure factor from the same data set. For highly ordered systems the results should be very comparable; for disordered systems some differences can be expected since Rietveld refinement does not have to simultaneously fit the diffuse scattering. On the other hand, Rietveld refinement is much, much faster!

Tucker *et al* have developed a hybrid method for modelling total structure factors [48, 49]. In this case they can simultaneously fit to $g(r)$, to $F(Q)$ (calculated via Fourier transform) and to the extracted elastic Bragg peak intensities (calculated via equation (11)). Although all of this information comes from the same data set, the results will differ slightly depending on the different weightings—$g(r)$ giving more emphasis to short-range order and elastic intensities to long-range order.

4.4. Direct calculation method for single-crystal materials

While it might seem at first that single-crystal data would be preferable to powder diffraction data, since they provide three-dimensional information rather than a one-dimensional average, in practice there are some difficulties.

- Single-crystal data can usually only be measured at a smaller number of Q-points in a restricted number of symmetry planes.
- They are much harder to correct and normalize on an absolute scale.
- The instrumental resolution affects Bragg peaks and diffuse scattering differently.
- Suitable samples are more difficult to produce.
- For neutron diffraction it is difficult to obtain consistent energy integration over the entire Q-range. The (incident-wavelength-dependent) intersection of the energy integration path and the phonon dispersion curves can lead to quite characteristic 'shapes' in the diffuse scattering.

The direct calculation method has been implemented for single-crystal neutron diffraction data in the RMCX program [11], but this has so far only been used to model diffuse neutron scattering data, and not Bragg scattering data. In addition an RMC refinement routine has been included in the diffuse scattering calculation program DISCUS which has been applied to both neutron and x-ray diffraction data [50–52].

5. Related methods

Before discussing other related methods of structural modelling, one general point must be made. Any method which produces a model which is in agreement with the available data is equally as valid as RMC modelling, and possibly more valid since it may for example include thermodynamic constraints, whereas RMC modelling does not. However, it is in fact rare that structural models which are not data based actually agree with the data within their errors, but it is not unusual for 'good agreement' to be claimed when the same level of agreement in an RMC model would be taken as indicating a serious problem! It should always be remembered that a suitable hard-sphere model will nearly always give a fair first approximation to a structure, so the success of any model should be judged relative to this. On the other hand, it should also be remembered that there is no simple linear relationship between 'goodness of fit' and 'goodness of model'.

5.1. Some other variations

As has already been discussed, the statistical sampling method used in RMC modelling has no particular significance—it is simply a means to obtain models that agree with the data. However, other authors have tried to 'improve' RMC modelling by modifying the statistical sampling. Toth and Baranyai have carried out a number of detailed tests, for example constraining the entropy, and find that this makes the program more efficient [53–55]. Such modifications may be useful, particularly for rather large models, but several points should be made.

- The 'standard' RMC algorithm is certainly rather inefficient, but this has been a deliberate policy in order to maximize its generality and ease of modification.
- New methods may have greater statistical validity in cases of ideal data. However, the biggest problem with real data is systematic errors, in which case the more sophisticated sampling methods may not be appropriate. New algorithms should therefore be tested on real data.

- Addition of such 'theoretical' constraints may give the impression that RMC modelling is indeed trying to obtain the 'correct' structure, whereas we have stressed that this is not the intention.

da Silva *et al* have used an approach where the radial distribution function is calculated from an ensemble of consecutive configurations [56–59]. These configurations are therefore correlated and hence this is not equivalent to either using a single very large configuration or multiple independent configurations. In addition they use a very small value of σ, which can result in essentially perfect agreement with the data (as long as the starting configuration is sufficiently close to the final result). This is claimed as an advantage of the method. While it may be so in the case of ideal data, there are few cases of real data where a perfect fit would be sensible (or even possible). Another claim is that the new algorithm does not require the use of '*ad hoc* constraints' such as atomic closest approaches. However, the imposition of a closest-approach constraint is exactly equivalent to using a set of data for which $g(r < r_0) = 0$ and $\sigma(r < r_0) \approx 0$, so in this respect it is identical to 'standard' RMC modelling. The formulation in terms of closest approaches is simply more transparent and physically understandable.

Adams and Swenson [60, 61] have introduced the possibility of constraining the bond valence sum calculated from a configuration into the RMCA program. This is similar to the inclusion of a simple form of potential. When applied as a relatively soft constraint it mainly has the effect of preventing some structural defects that might otherwise occur on a statistical basis. However, the bond valence of the final models can then be used self-consistently to calculate, for example, ion conduction pathways (see section 7.2). A similar constraint has been implemented in the RMCPOW program [62].

5.2. Metropolis Monte Carlo (MMC) simulation and other Monte Carlo methods

The method most obviously related to RMC modelling is MMC simulation. Whereas RMC modelling requires data, MMC modelling requires an interatomic potential. MMC modelling is therefore thermodynamically consistent but may not agree with experimental data, while RMC modelling agrees with data but is not thermodynamically consistent. In general MMC modelling is not widely used for producing structural models of 'real systems', but is widely used for making rather large statistical models of 'idealized systems', e.g. substitutional alloys or magnetic Ising models. MMC modelling is also used in a number of potential refinement methods, as discussed in the next section.

Two further Monte Carlo methods should be mentioned because they are sometimes confused with RMC modelling. The inverse Monte Carlo method [17, 18] is a very specific method for deriving effective pair interaction energies in binary alloys, based on structural models which are themselves determined by the Monte Carlo method of Gehlen and Cohen [63] from short-range-order parameters derived from diffuse scattering data. 'Simulated annealing' refers to a general Monte Carlo method for attempting to reach the global minimum of the function being sampled [64]. For example in MMC modelling one might wish to find the global energy minimum (true ground state) of the system being simulated. This is achieved by gradual reduction of the control variable, in this case the temperature, from a high value—hence the name given to the method. While simulated annealing is occasionally used in RMC modelling to avoid a local minimum with an unacceptably high value of χ^2, it must be stressed again that there is no global minimum in RMC modelling. Any configuration with a suitably low value of χ^2 is a valid configuration. The configuration with the lowest χ^2 can actually be worse since it clearly fits to details of the data errors.

5.3. *Potential refinement methods*

A number of methods have been developed which produce structural models from experimental data, but via the refinement of an interatomic potential (e.g. [65–70]). Probably the most extensively used of these is the empirical potential structure-refinement (EPSR) method due to Soper [68]. At first it seems that such methods must better than RMC modelling, since the models should agree both with the data and with a potential. However, some caution is required in this respect.

Potential refinement methods all work in the same basic manner. A starting potential is used to generate a structure, e.g. via MMC modelling, and calculate for example a structure factor. This is compared to experimental data. The difference in structure factors or radial distribution functions is then used to generate a modified potential and the scheme is iterated. When the calculation and experiment agree within the required limits, the potential can then be used to generate multiple configurations (all agreeing with the data), which can be used to calculate for example many-body correlations with high statistical accuracy, as shown in figure 3. The statistical sampling and thermodynamic consistency are certainly better than with RMC modelling, and the use of a potential also prevents some structural defects. However, several questions must be asked.

- Does the use of a potential with a specific functional form bias the model that fits the data, and what happens if the form is inappropriate? It is clear that there must be some bias. In many cases, where the system can be described by an effective two-body potential, this is probably not a problem, but where many-body forces are significant (which does not necessarily mean that they are large) the bias may prevent certain atomic configurations. However, there is of course no guarantee that RMC modelling will do better. For systems close to a transition where the local potential energy may fluctuate significantly, e.g. a metal–insulator transition, the imposition of a simple global form of the potential might give bad results. (The same would also apply to any simulation using a simple global potential.)
- Can the potential derived be used for any other purpose than producing a structural model, for example in a molecular dynamics simulation? Here the answer is, probably not. In a simple case such as modelling liquid argon based on a Lennard-Jones potential, where it is already known that the potential form is suitable and there are only two parameters to derive, it would be surprising if there was a problem. However, Soper [34] has performed a series of test studies which show that a variety of potentials can be generated, both in atomic and molecular systems, which reproduce the original structure factors and even the original three-body correlations, i.e. that give an equally good representation of the structure. This suggests that derived potentials, at least those based on methods developed so far, are useful as a tool within the structural modelling program, but should not be used outside of it.

It should be remembered that if a suitable form and initial parameters are chosen for the potential, the resulting structure factor may well agree with the available data even if it contains large errors (e.g. [71]). Poor or limited data only contain limited information, and there is no method that can extract more information than is provided. It can also be noted that the effect of certain types of data error gives predictable results in RMC models, for example a sloping background at high Q often gives a sharp spike or cut-off at low r in $g(r)$. The imposition of a potential form will spread these effects in a less predictable fashion.

With these caveats in mind it is clear that for modelling the structure of many liquids, a method such as EPSR has sufficient advantages over RMC modelling that it should be

recommended. There is less experience with glass structures, though metallic glasses are almost certainly suitable subjects since they are rather close to hard-sphere systems. Whether the method is useful for crystalline materials is not known. The differences between the methods can be summarized in the following way—RMC modelling is more general and hence can be applied to almost any system, EPSR is more specific and will provide better results in appropriate cases.

5.4. Molecular dynamics simulation

Classical molecular dynamics (MD) simulation requires an input interatomic potential. Like MMC modelling it is thermodynamically consistent, with the obvious major advantage that both structure and dynamics can be studied. If the MD simulation reproduces the experimental structural data, then it is without doubt the most appropriate method. If there are differences, then the simulation is not necessarily invalid—this entirely depends on the level of difference and the purpose of the simulation. MD modelling can also be tested by comparison with dynamical information, e.g. diffusion constants, phonon dispersions or vibrational density of states.

Methods of *ab initio* molecular dynamics simulation, such as the Car–Parrinello method [72], are in principle potential independent, giving a full quantum mechanical treatment to the electrons. In practice only the valence electrons are treated this way and pseudopotentials are used to describe the core electrons. The method is highly computationally expensive, so system sizes are typically limited to under 100 atoms and run times to a few ps. Finite-size effects may therefore be significant, though some techniques have been developed that allow more realistic comparison with experimental structural (and dynamical) data [73]. Some simulations have shown reasonable agreement with experiment but some have shown serious discrepancies. Despite this, a major advantage of the method is that it can give information on the valence electron distribution, i.e. on bonding, particularly in cases where there are significant local fluctuations. An example is given in section 6.2.

In general it can be considered that MD simulation and RMC modelling are complementary methods—they may sometimes address the same problem but in different ways. A recent approach is to use RMC modelling to help in refining potentials for improving the agreement between MD simulation and experiment (e.g. [74]).

6. RMC modelling of liquids

6.1. Metal–insulator and metal–semiconductor transitions in elemental liquids

A 'classical' analysis of liquid structure data involves determination of the radial distribution function and then interpretation of peak positions and average coordination numbers. Sometimes this reveals very little. In the case of expanded Cs, for example, there is an interest in the metal–insulator transition that takes place in the vicinity of the critical point. Structural studies along the coexistence curve show a first-peak position that varies very little as a function of decreasing density and an average coordination number that has a remarkably linear decrease [75]. However, RMC modelling is able to show that at low densities these features imply a structure within which the average coordination 'hides' a considerable non-uniformity in the local atomic distribution, with a wide variation in coordination number [76]. The metal–insulator transition appears to be related to a percolation transition in the Cs 'bonding network' [77]. The situation in Hg is somewhat different. Here it is possible to identify two different local coordinations which may be associated with 'metallic' and 'covalent' bonding

environments [78]. At high densities the metallic bonding network dominates and so the system is overall metallic. At intermediate densities there are interpenetrating metallic and semiconducting networks, so the net result is still metallic. The metal–semiconductor transition occurs at low densities due to a percolation transition in the metallic bonding network [79]. This is illustrated in figure 5.

6.2. Polyanions in liquid-metal alloys

One of the more controversial RMC studies of liquid structure concerns the possible existence of polyanions, or 'Zintl ions', in liquid-alkali–Pb and related alloys [80]. The basic idea is that in KPb, for example, the alkali can donate electrons to the more electronegative Pb, which then form Pb_4^{4-} tetrahedral clusters ('Zintl' ions) which are isoelectronic with the stable P_4 molecule. This would explain the sharp increase in (electronic) resistivity for K_xPb_{1-x} alloys at the equimolecular composition. Zintl ions are found in the equivalent crystal structures. Some evidence for clustering comes from diffraction data which are consistent with a Pb–Pb coordination close to three and show a strong 'first sharp diffraction peak' (FSDP) in the structure factor at $\sim$1 Å^{-1}, which was suggested to be due to intercluster correlations [81]. Molecular dynamics simulations and other theoretical calculations that included tetrahedral Pb_4 clusters gave reasonable quantitative agreement with diffraction data. However, thermodynamic calculations suggested that the proportion of Pb in tetrahedra should be only about 25% close to the melting point, and decrease rapidly with increasing temperature.

RMC modelling of a single structure factor from neutron diffraction agreed independently that the FSDP was associated with Pb [80]. This by itself can be identified as a definite success for RMC modelling, since there is no reason *per se* why it could not also have identified it as due to K, having no prior knowledge of the likely bonding. (Similar results were obtained for a number of other systems (e.g. [82])). By the use of varied coordination constraints it was possible to show that models with a range of Pb_4 tetrahedra between 25% and 100% were consistent with the data. The former model could be better characterized as a predominantly threefold-coordinated Pb network.

Here it is useful to make another specific point concerning what is, or is not, shown by specific features in diffraction data. Even as recently as 1999, Hafner *et al* [83] stated 'However, so far reverse Monte Carlo calculations agree only on the existence of a certain fraction of polyanions, but in a much smaller number and with less perfect structures than the sharpness of first sharp diffraction peaks in the static structure factors would suggest'. However, this is illogical. Since the RMC models fit the data, they reproduce the sharpness of the FSDP, so the FSDP does not *necessarily* suggest a large number of perfect Zintl ions.

So did RMC modelling make any useful contribution, being only able to say that the Zintl ions might exist, but then again they might not? The answer must be yes, particularly by indicating that a number of solutions were possible. Studies using *ab initio* MD simulation [84, 85] (in which it is not necessary to pre-decide on Pb_4 units, as it is with classical MD modelling) supported the idea of a more network-like structure, with an atomic arrangement that was remarkably consistent with the unconstrained RMC model. Later work [86] showed how electrons could localize preferentially around tetrahedral groupings, in this case Sn_4 in KSn, even though there were also other Sn in the local region which would be identified as being coordinated to the same grouping. Related work shows that individual polyanions may only have a relatively short lifetime, of order a few ps; i.e. they are not 'molecules' [87]. However, the electron thermalization is much faster than 1 ps, so as long as there are on average a high percentage of polyanions at any time, then there will be a high degree of electron localization and a high resistivity. Figure 6 shows two pictures of Pb atoms from an unconstrained RMC

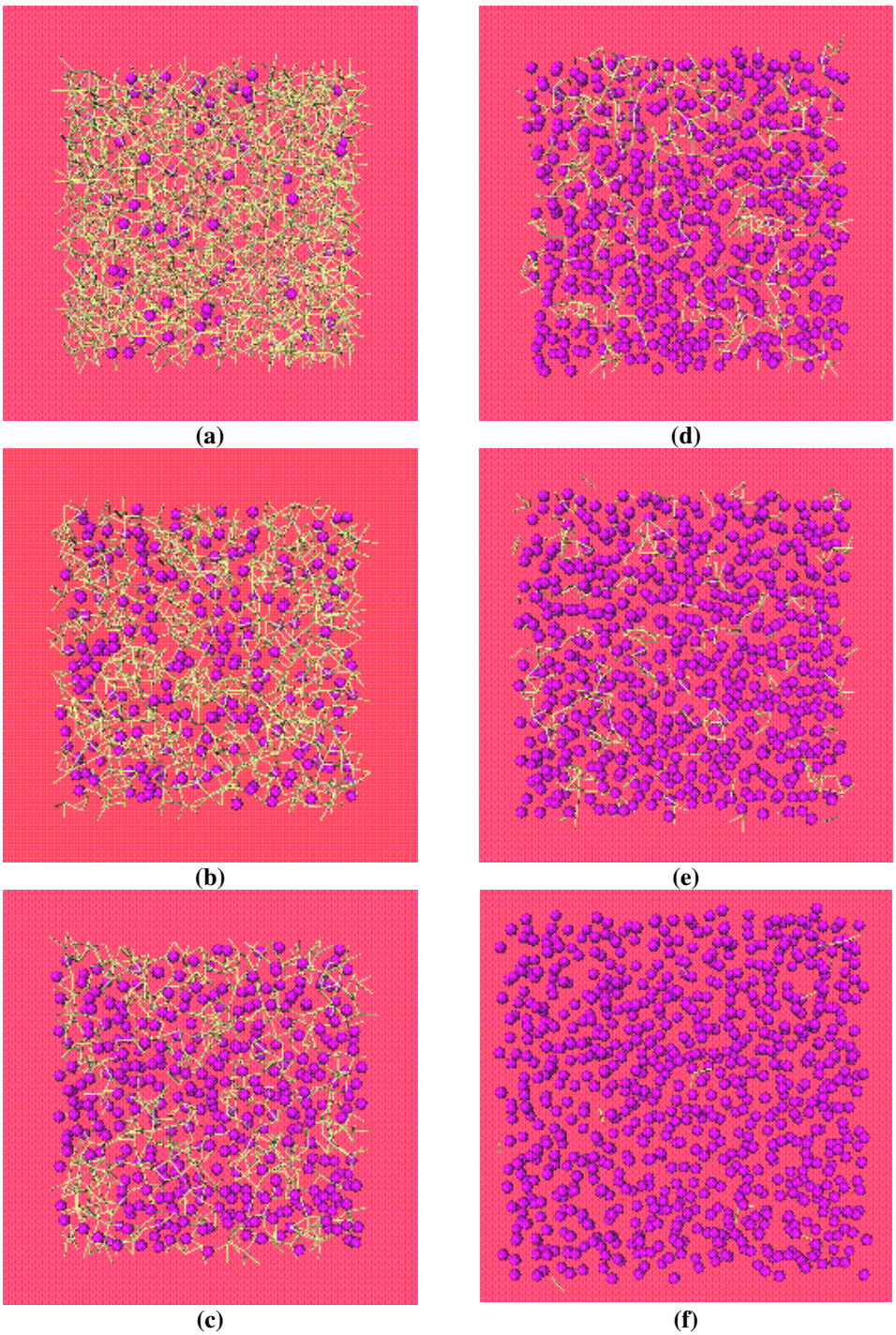

Figure 5. 10 Å thick sections of configurations for expanded Hg at (a) 293, (b) 773, (c) 1073, (d) 1473, (e) 1673 and (f) 1803 K. Semiconducting atoms and metallic bonds are drawn as balls and sticks respectively [79].

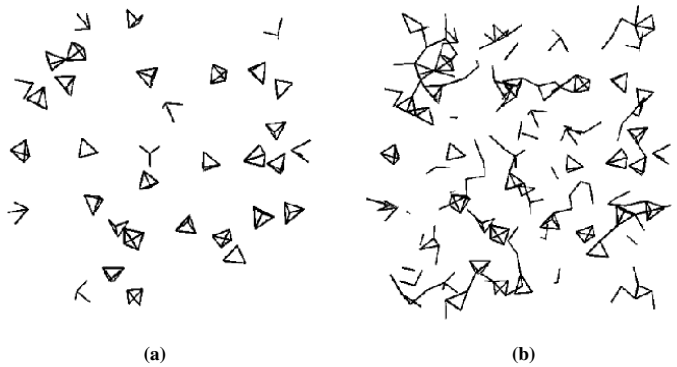

Figure 6. Pb atoms only from a section of an RMC model for KPb at 873 K [80]. (a) Bonds between Pb atoms less than 3.6 Å apart in identifiable tetrahedral clusters. (b) Bonds between all Pb atoms less than 3.6 Å apart. Note that bonds are only drawn from atoms within the section, so some tetrahedra appear 'incomplete'.

model for liquid KPb. In one case the 'picture' is of isolated tetrahedra, consistent with a high resistivity, while in the other case the picture is of a network, but the model is the same. This illustrates how apparently different ideas can be consistent with a single model.

7. RMC modelling of glasses

7.1. Vitreous silica and silicates

RMC modelling of glass structures has developed continuously and can be well illustrated by the example of vitreous silica. The early model of Keen and McGreevy [7] used no coordination constraints, but was the first to combine neutron and x-ray diffraction data. Later on, coordination constraints were introduced by Wicks and McGreevy [22] and additional bond-angle constraints by Keen [27]. The most recent work by Kohara [28] uses high-Q-range neutron and hard-x-ray diffraction data; the quality of the data is clear from the very sharp and well defined peaks in the partial radial distribution functions, as shown in figure 2. For alkali silicates the results of magic angle spinning NMR measurements were incorporated into the models [22] to provide the proportions of Q_n species, that is of Si with n non-bridging oxygens. Recently, combined RMC/MD studies have been used for modelling rather complex oxide glasses [74].

7.2. Fast-ion-conducting glasses

Probably the consistently most successful application of RMC modelling has been in the study of fast-ion-conducting glasses [88]. It is useful and interesting to follow this from a historical perspective, since it illustrates rather well many of the particular advantages of RMC modelling.

By adding Ag or Li halides to 'traditional' glass formers such as $(Ag_2O)_x(B_2O_3)_{1-x}$ or $AgPO_3$ it is possible to produce glasses with a high ionic conductivity. These have possible applications in e.g. microbatteries. However, the glass transition temperature, T_g, tends to be lower when the conductivity is higher, and if too much salt is added, eventually crystallization occurs and the high conductivity is lost. The questions to be answered are therefore (a) what causes the high conductivity and (b) is it possible to increase T_g or correspondingly the glass formation range? In addition, the first neutron diffraction studies [89] showed the existence

of a sharp peak in the structure factor at an anomalously low Q-value, 0.7–0.8 Å^{-1}, whose intensity appeared to be correlated with the AgI content and hence with the high conductivity. This aroused considerable interest.

Initially it was considered that an RMC model based on a single neutron diffraction pattern would be unreliable for a four-component glass, e.g. $(AgI)_x(AgPO_3)_{1-x}$, since conventionally ten separate measurements are required to obtain the ten partial structure factors. This ignored the power of constraints. The structures of crystalline analogues contain polymeric phosphate chains, with two bridging and two non-bridging oxygens, cross-linking occurring via ionic bonding, so the initial configurations were built containing such chains, using a method similar to that outlined for potassium silicate in section 2.4. This is illustrated in figure 7.

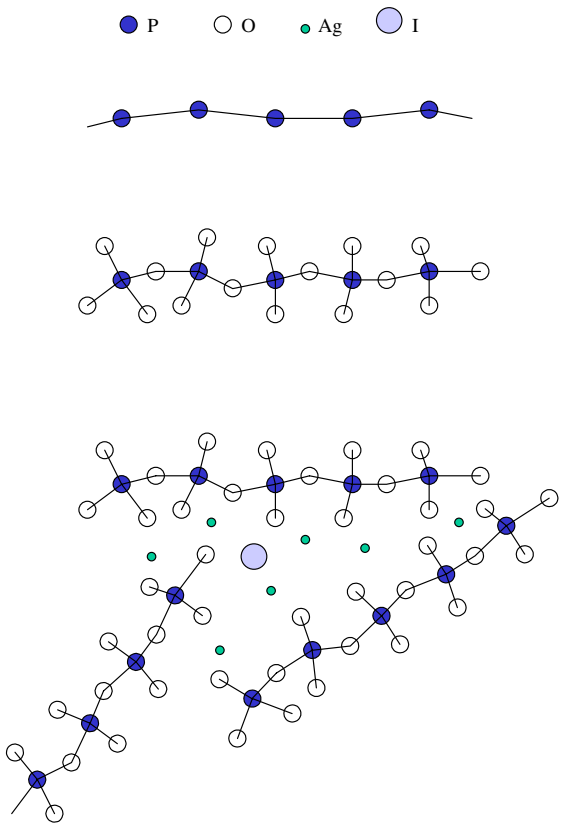

Figure 7. Steps in the creation of an initial RMC configuration for $(AgI)_{0.5}(AgPO_3)_{0.5}$ glass [24]. Firstly CHSMC is run for P atoms only with a twofold-coordination constraint. This creates a configuration of P chains. Bridging O atoms are added at P–P bond centres and two non-bridging O close to each P atom. CHSMC is run with a fourfold P–O constraint until all cut-offs are satisfied. Finally Ag and I are added at random and CSHMC is again run until cut-offs are satisfied. The resulting configuration shows a FSDP even before RMC fitting.

Even before fitting to the data, at the number density corresponding to $(AgI)_{0.5}(AgPO_3)_{0.5}$, a FSDP was found, while at the (lower) density corresponding to $AgPO_3$ there was no FSDP, in accord with experiment. However, the FSDP occurred in the partial structure factors corresponding to P–P, P–O and O–O pairs, whereas the explanation in the literature was that it was due to AgI clustering and hence should be related to Ag and I correlations. This

could be tested in a very simple way. Neutron diffraction is dominated by P and O scattering, whereas x-ray diffraction is dominated by Ag and I. If the RMC model was correct, then x-ray diffraction should show a weak FSDP, whereas if RMC modelling was wrong, it should show a very strong FSDP. The experiments confirmed the RMC prediction. The correlation of FSDP intensity and AgI content was explained by the fact that adding AgI 'pushes apart' the phosphate chains, which gives rise to the FSDP. Finally a combination of neutron diffraction, x-ray diffraction, Ag K-edge EXAFS and I L_{III}-edge EXAFS was used to make models for a series of glasses [24] (with the later addition of phosphorus NMR data [23]).

The RMC models were used to investigate the distribution of free volume available for Ag^+ conduction—i.e. conduction pathways. As the salt content increased, the connectivity of the conduction pathways also increased, giving higher conductivity, but the degree of cross-linking between phosphate chains decreased, lowering T_g and leading eventually to crystallization. Hence it could be suggested that it would effectively not be possible for this class of materials to obtain significantly higher conductivity at the same T_g, or higher T_g at the same conductivity. This prediction has not been disproven by any subsequently produced glass. Swenson and Börjesson [90] extended the free-volume argument to show that the conductivity can be predicted from the densities of the doped and undoped glasses for a wide variety of systems.

From the RMC models it was found that almost all Ag occur in mixed (P, O and I) environments, so there is almost no atomic arrangement that could be described as an AgI cluster. If constraints were applied to increase clustering, then the data could not be fitted properly. Strangely, despite the fact that the RMC prediction of the origin of the FSDP was confirmed quite clearly, as described above, and a number of subsequent studies on a wide range of glasses have produced consistent results [88], there are still papers published in the literature which assign the FSDP to AgI clustering, though mainly on the basis of data which are relatively indirectly linked to the structure (e.g. [91]).

The most recent development has been the use of bond valence constraints. Adams and Swenson [61] have applied these to a number of different glasses, producing basically similar models but with the added consistency of a physically reasonable bond valence, and a smaller number of 'structural defects'. 'Free-volume' pathways then become 'bond valence' pathways for ionic conduction, which can be used to make more quantitative predictions. An excellent quantitative agreement between the RMC models and the measured ionic conductivities is then found [60]. Figure 8 shows the Ag^+ conduction pathway for $(AgI)_{0.6}$–$(Ag_2O$–$2B_2O_3)_{0.4}$.

8. RMC modelling of disorder in crystals

As discussed in section 4.3, the application of RMC modelling to single-crystal diffraction data has so far been somewhat problematic and there have been relatively few applications. The most detailed work has been a study of ice by Nield *et al* [92–95] using the program RMCX and of stabilized zirconias by Proffen and Welberry [96–98] using the program DISCUS.

There have been numerous RMC studies of crystalline fast-ion conductors using powder diffraction data, primarily Ag and Cu halides and chalcogenides [42, 99–103]. In one case RMC modelling, experiment and MD simulation have been compared in detail [104]. More recently there has been a very detailed study of disorder in the various crystalline polymorphs of SiO_2 [49, 105], where now the atom positions are constrained by the covalent Si–O bonding network. Another type of disorder that can be modelled is the rotational disorder of molecules. Here we give two examples—both of which give rather clear conclusions.

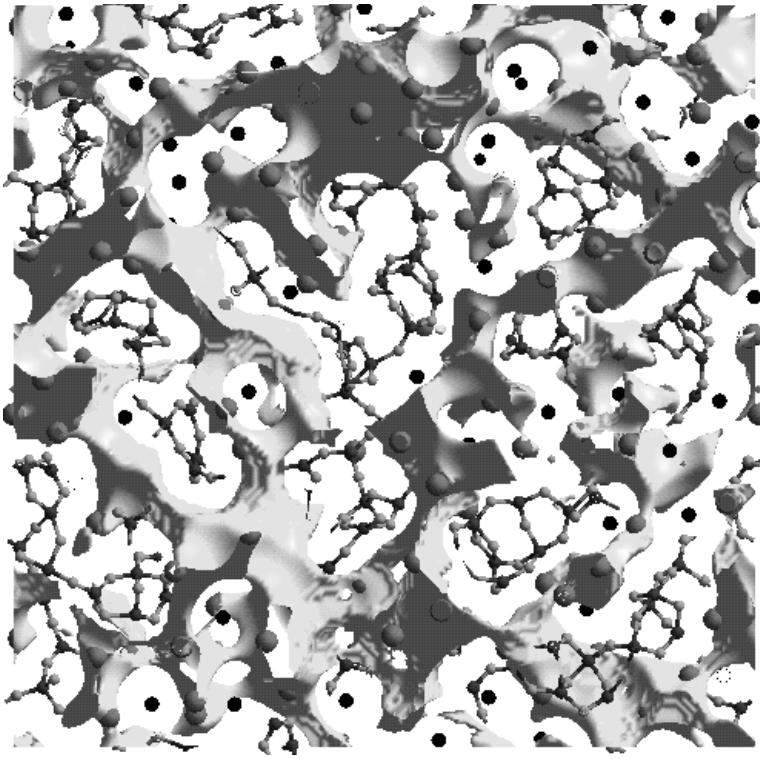

Figure 8. A 5 Å thick section through the Ag^+ bond valence isosurface for an RMC model of $(AgI)_{0.6}$–$(Ag_2O$–$2B_2O_3)_{0.4}$ glass [61]. Ag—large grey spheres; I—black spheres; borate is shown as a network with small spheres for B (dark grey) and O (light grey).

8.1. Rotational disorder

One of the simplest illustrations of the use of RMC modelling in crystals is a study of rotational disorder in NH_4Cl, or rather its deuterated analogue ND_4Cl [106]. Cl^- ions form a simple cubic structure. The tetrahedral ND_4^+ occupy the cube centres and hence can (on average) have two equivalent orientations (figure 9(a)), between which they can rotate at higher temperatures. Two questions arise: how do they rotate and are there correlations between the orientations of neighbouring ND_4^+?

The RMC model shown in figure 9 has been obtained by fitting to the total structure factor as measured by means of neutron diffraction (figure 4) using the convolution method (section 4.2). It can be used to answer these questions very easily. Note that the $2 \times 4 = 8$ D positions in figure 9(a) form the corners of a cube. If you look carefully in figure 9(b) you can see the orientations of individual ND_4^+. No particular correlations are found between neighbouring ions. Figure 9(c) shows that there are a variety of orientations, not just those shown in figure 9(a). This is of course obvious—if the ions rotate, then they must spend at least some time at 'intermediate' orientations and in addition there are 'normal' thermal vibrations. Figure 9(d) shows this more clearly, but also shows that the D distribution is not completely spherical, so the 'intermediate' orientations are less common than the 'equilibrium' orientations of figure 9(a). Figure 9(e) then shows that the most likely path between the 'equilibrium' orientations is approximately along the 'edges' of the D 'cube'. D positions on the 'faces' of the 'cube' are rare. Translated into more scientific language, this means that

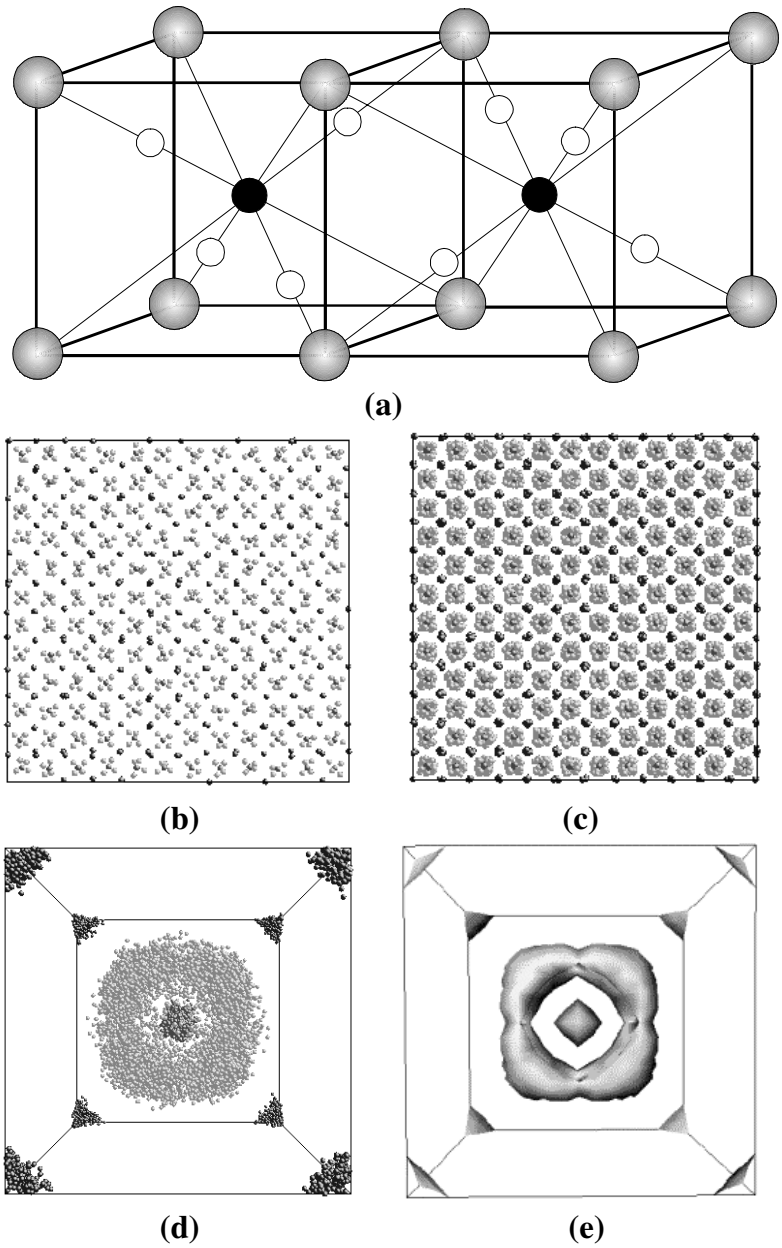

Figure 9. Different views of the 'structure' of ND_4Cl [44]. (a) 'Conventional' crystal structure showing the two ND_4^+ orientations. (b) A 10 Å thick slice from an RMC model of 10 368 atoms ($12 \times 12 \times 12$ unit cells). (c) A projection of the whole model. (d) As (c), but individual atoms are now translated into a single unit cell. (e) An isodensity surface of the distribution shown in (d). The D density is 0.27 of its maximum value.

ND_4^+ rotate preferentially about twofold axes, with less than 5% rotating about threefold axes. A similar study of ND_4I has compared RMC modelling and maximum-entropy reconstruction methods [107].

8.2. Proton conduction

A more complex example also concerns rotational disorder, but now coupled with diffusion. The 'paddle-wheel' model was developed many years ago to explain ion conduction in Li_2SO_4 [32]. The basic idea is that as SO_4^{2-} ions rotate, they carry with them the small Li^+ ions; i.e. rotation and diffusion are highly correlated. This led to arguments stretching over nearly two decades, since others believed that uncorrelated diffusion (percolation) could also explain the experimental results [104]. The 'paddle-wheel' model was invoked to explain many other systems, sometimes under different names such as the 'turnstile mechanism'. For example the model was used to explain proton conduction in $CsHSO_4$ on the basis of quasi-elastic neutron scattering (QENS) data [105].

Figure 10 shows results from an RMC model of $CsDSO_4$ [106]. Although the SO_4^{2-} ions are very disordered due to their rotations and vibrations, a preferential orientation can still be identified—clusters of O positions can be seen forming the vertices of tetrahedra (figure 10(a)). The D distribution is also highly disordered and follows a curved path very similar to that proposed on the basis of QENS data. One thing that is immediately obvious is that the D pathway intersects strongly with the O positions occupied when the tetrahedra are rotating. Since D and O cannot be in the same place at the same time, rotation and diffusion must be correlated.

Figures 10(b), 10(c) show the partial radial distribution function, $g_{OD}(r)$. The first peak occurs at the same distance at high and low T, which is the same as the shortest O–D distance in the time-average low-T structure, but not in the time-average high-T structure. Actually from figure 10(a) it is clear that the high proton diffusion rate at high T makes it completely meaningless to try to define a time-average D position—D will always spend more time away from such a position than at it. The other thing to note is that the peak in $g_{OD}(r)$ is still sharp at high T (in fact even sharper than at low T), despite the high level of disorder in both O and D positions shown in figure 10. This means that not only are SO_4^{2-} rotations and D^+ diffusion correlated—they are highly correlated! For the majority of the time they must effectively exist as DSO_4^- ions, with individual D being exchanged between chains of neighbouring ions in a way that is also highly correlated—a 'multi-paddle-wheel' mechanism.

It is interesting to note that a similar study of Li_2SO_4 concluded that the rotation/diffusion correlation was much weaker—effectively both 'paddle-wheel' and 'percolation' mechanisms operated with approximately equal probability [32]. This explains the long-running controversy—both were right!

9. RMC modelling of magnetic structures

9.1. Metallic glasses

In the same way that RMC modelling can be used to model an atomic structure, it can also be used to model a magnetic structure, except that now two models are required—one of atoms and the other of magnetic moments which are associated with some of the atoms. In order to fit the data, the atoms must be moved (which can alter the position of the magnetic moments and hence changes both the atomic and magnetic scattering) and moments must be rotated (which only changes the magnetic scattering). For modelling magnetic glasses a Fourier transform method is used, similar but not identical to equation (2). This is implemented in the program RMCSPIN [10].

The first such RMC study, of $Dy_{0.7}Ni_{0.3}$ glass [10], used neutron diffraction data which had been measured with 'double-null' isotopic substitution [112], taking advantage of the special

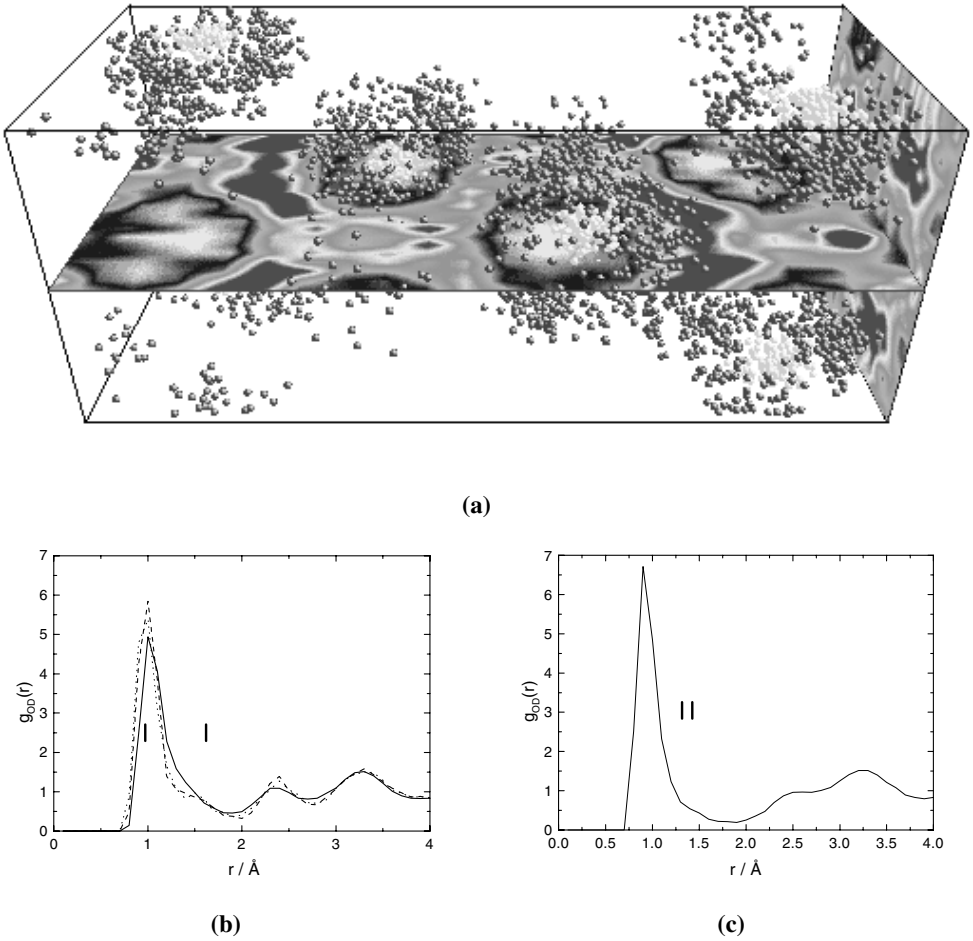

Figure 10. (a) An RMC model of the high-temperature proton-conducting phase of $CsDSO_4$ [106]. The individual atom positions in a 5376-atom ($8 \times 8 \times 3$ unit cell) model have been translated into a single unit cell—S are light grey, O are dark grey and Cs are not shown. The D density distribution is represented as a contour plot in two planes. (b) $g_{OD}(r)$ for $CsDSO_4$ in the non-conducting phase at 295 (solid curve), 333 (dashed curve) and 373 K (dotted curve) and (c) in the conducting phase at 412 K (solid curve). Bars indicate O–D distances determined from the respective time-average crystal structures.

circumstance that both Dy and Ni have isotopes with both positive and negative scattering lengths. This enabled rather uniquely the direct experimental separation of the atomic and magnetic scattering, making modelling much easier. Later studies of $(Dy_{1-x}Y_x)_{0.7}Ni_{0.3}$ [113, 114] and $Dy_{0.7}Fe_{0.3}$ [115] used the fact that these glasses were approximately structurally isomorphous with $Dy_{0.7}Ni_{0.3}$ and hence could use the same structural model. One general result from these models was that the magnetic structures were rather more disordered than had been expected, but by including local constraints on the magnetic structure it could be shown that significantly more ordered models would not be consistent with the data. The angular correlation function for magnetic moments, $\langle \boldsymbol{\mu} \cdot \boldsymbol{\mu} \rangle_r$ (equivalent to the radial distribution function for atomic structures), cannot be derived directly from the measured scattering because of the form of the relevant equations, but only on the basis of a three-dimensional structural

model, e.g. RMC modelling. For these glasses $\langle \boldsymbol{\mu} \cdot \boldsymbol{\mu} \rangle_r$ has a highly oscillatory form very similar to that predicted for a RKKY interaction.

$Fe_{0.91}Zr_{0.09}$ glass was modelled on the basis of neutron and x-ray diffraction data (including anomalous scattering) [116]. In this case $\langle \boldsymbol{\mu} \cdot \boldsymbol{\mu} \rangle_r$ is relatively flat, as expected for long-range ferromagnetic order. This study has highlighted the role that the variation in local (nearest-neighbour) structural environment, which is an inherent feature of the essentially random close-packed structure, can play in determining the magnetic interactions and structure in magnetic glasses on a wide range of length scales. On the basis of the RMC model for a single composition, it was possible to predict the variation of the magnetic phase diagram as a function of composition. Some results are illustrated in figure 11.

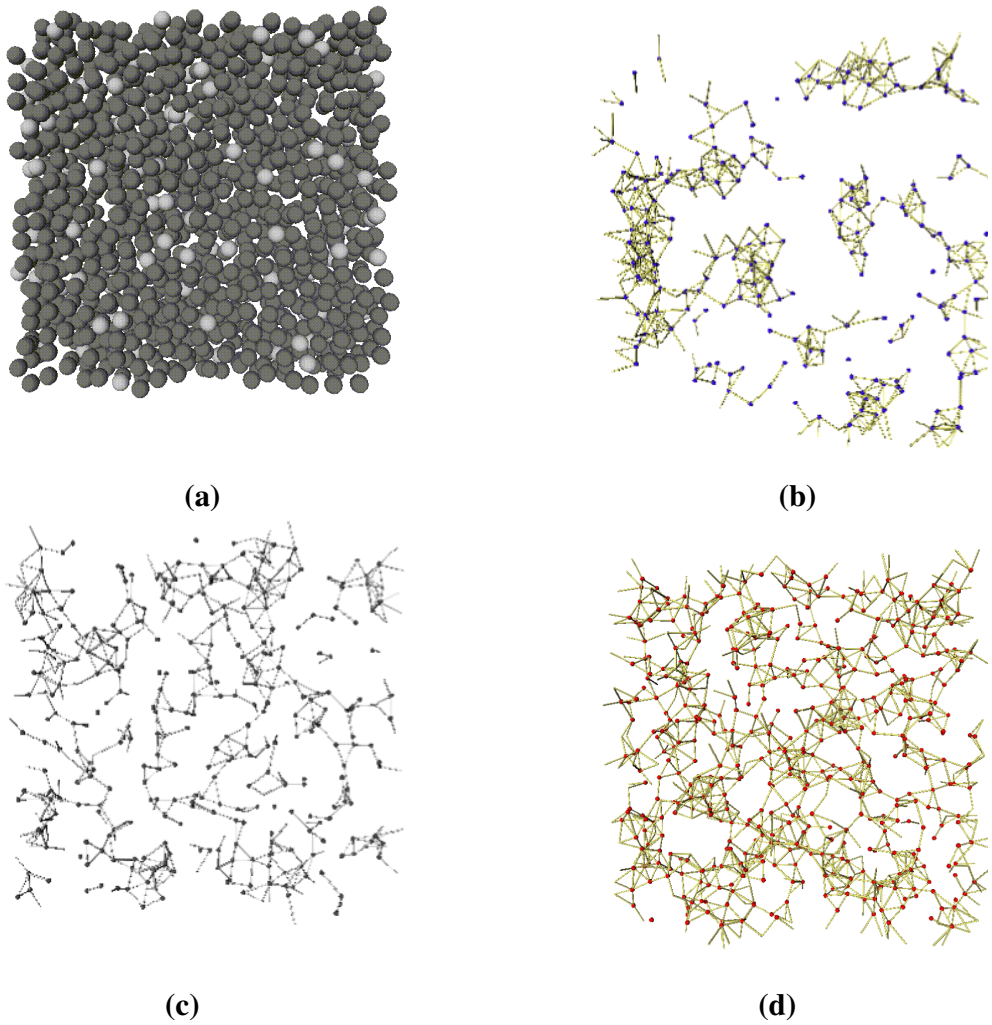

Figure 11. RMC models for $Fe_{1-x}Zr_x$ glasses [116]. (a) $x = 0.09$. Fe atoms (dark grey), Zr atoms (light grey). (b) $x = 0.09$; bonds are drawn between neighbouring Fe atoms in locally anti-ferromagnetic environments. (c) $x = 0.75$; (d) $x = 0.6$; bonds are drawn between neighbouring Fe atoms in locally ferromagnetic environments.

9.2. Colossal-magnetoresistance (CMR) materials

RMC modelling of crystalline magnetic materials cannot use the Fourier transform method, and must be done via direct calculation (equivalent to equation (9)). This is implemented in the RMCPOW program [13, 117].

CMR materials have been known about for almost 40 years, but in the last decade there has been a revival of interest due to the realization that thin films could be made with the potential for applications in devices such as magnetic recording heads. Various experimental and theoretical studies have invoked a variety or combination of mechanisms to explain their extreme properties—double exchange, lattice polarons, magnetic polarons, spin–lattice coupling etc.

Some results from a structural model for the CMR material $La_{0.8}Sr_{0.2}MnO_3$ are shown in figure 12 [118]. It is worth stressing that the average structure of this model is completely consistent with that determined from Rietveld refinement, and with other studies in the

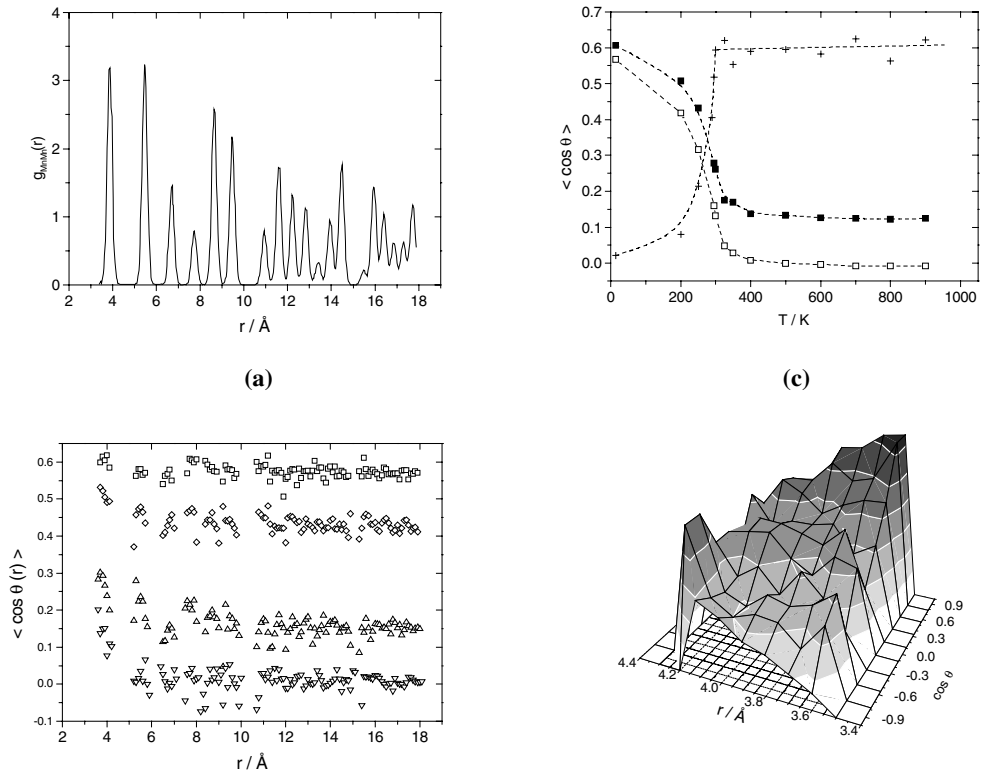

Figure 12. Various correlations relating to magnetic ordering in $La_{0.8}Sr_{0.2}MnO_3$ [118]. (a) The radial distribution function for Mn atoms, $g_{\mathrm{MnMn}}(r)$. (b) The average cosine of the angle between magnetic moments on Mn atoms as a function of their separation at 15 (downward-pointing triangles), 200 (upward-pointing triangles), 300 (diamonds) and 900 K (squares). (c) Variations of short-range lattice distortion (crosses), short-range magnetic order (closed squares) and long-range magnetic order (open squares) as a function of temperature. Dashed curves are drawn as guides to the eye. (d) The spin–spin cosine distribution function, $p(\cos\theta(r), r)$, at 325 K. Only distances corresponding to Mn–Mn near neighbours, $3.4 < r < 4.4$ Å, are shown.

literature. The radial distribution function for the magnetic Mn atoms (figure 12(a)) shows the distances between magnetic moments. The average cosine of the angle between moments as a function of distance (figure 12(b)) has a high value at low T where there is long-range ferromagnetic order (0.6 is close to the predicted quantum mechanical expectation value). As T increases above the magnetic ordering temperature, the cosine decreases to zero at long distances but remains finite at short distances, indicating that short-range magnetic ordering remains (magnetic polarons). At the same time there is the onset of short-range lattice disorder (lattice polarons) which can be monitored through the width of the first peak in $g_{\mathrm{MnO}}(r)$ (figure 12(c)).

These results show that lattice and magnetic polarons coexist at high temperatures. However, the model can reveal even more subtlety. If you look carefully at figure 12(b) you can see that at high T the average cosine actually rises steeply as r decreases for distances within the first peak of $g_{\mathrm{MnMn}}(r)$. The full cosine distribution function, shown in figure 12(d), explains this. When two Mn moments are slightly closer together they have a higher probability of being ferromagnetically aligned ($\cos\theta = 1$), giving the peak at the back right in the distribution. If they are slightly further apart they have a higher probability of being antiferromagnetically aligned ($\cos\theta = -1$), giving the peak on the front left. Lattice and magnetic polarons are therefore coupled—indeed they are one and the same. In the case of $La_{0.67}Ca_{0.33}MnO_3$ [119, 120] the variation between the strengths of the local ferromagnetic and antiferromagnetic alignments is greater. The local antiferromagnetic ordering is strongest just above T_c, with a clear correlation with a local orthorhombic lattice distortion, before the local ferromagnetic ordering 'wins' and long-range order sets in. It should be emphasized that RMC modelling is unique in its ability to model this type of local lattice/magnetic order.

9.3. Magnetic structure determination

It turns out that the RMCPOW program is also a useful tool for aiding *ab initio* determination of (time-average) magnetic structures from powder diffraction data [121]. An example is shown in figure 13. In this case only the Bragg peaks are fitted and a small model is used, chosen to be consistent with possible magnetic supercells. The method has two main advantages. Firstly it can start from a random initial structure, so no prior idea or knowledge is required. Secondly it may be possible to find more than one spin structure which is consistent with the data. These can either be distinguished on the basis of other available information, or used to suggest further experiments that might distinguish them, e.g. single-crystal or higher-resolution studies.

10. Future developments

10.1. RMCA

The RMCA program has now been in use for almost ten years, with only minor modifications. Some improvements are required of the methods for dealing with EXAFS data [122], which have been used relatively little, and it would make sense to combine RMCA and RMCSPIN programs. There is a general trend towards the use of larger structural models that would be helped by including techniques for improving efficiency, e.g. link cell methods such as are used in large MD models. Otherwise it is the extension towards new data types that would be of most interest. For example, the ability to include different types of NMR data, infrared absorption data or Raman scattering data could be extremely powerful. However, this is hampered by the theoretical problems of calculating appropriate coupling constants, rather than the implementation in RMC modelling.

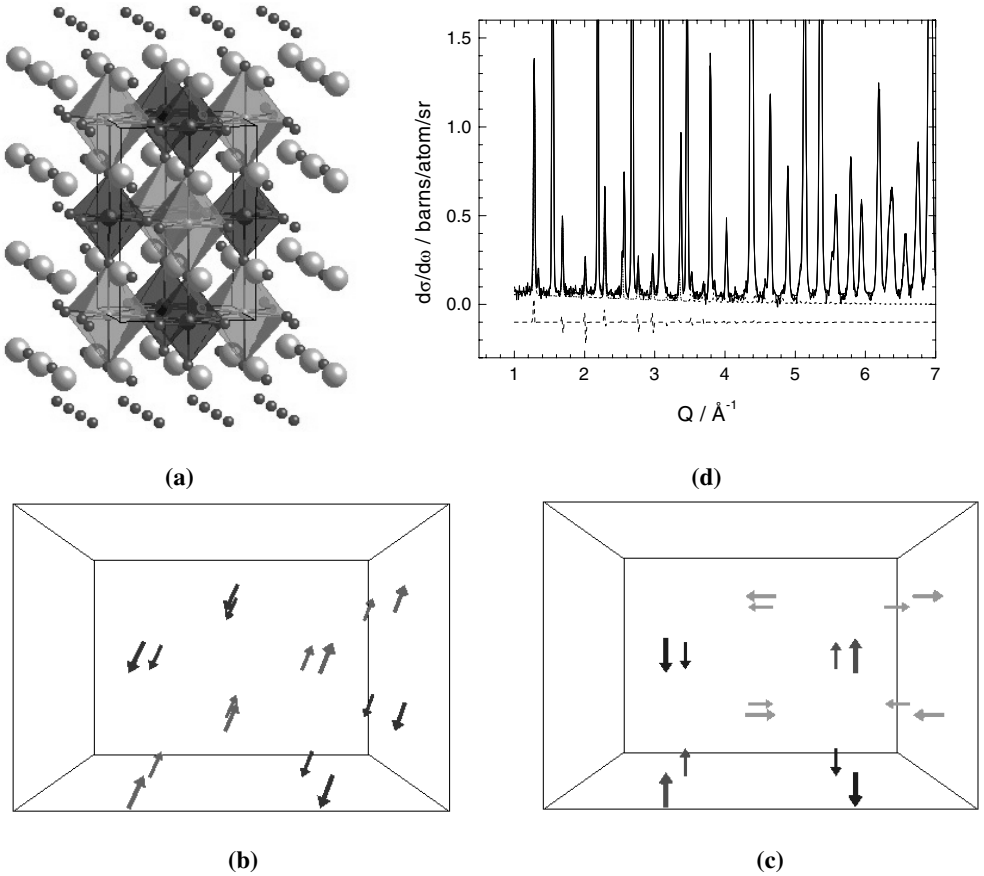

Figure 13. (a) Time-average crystal structure of the double perovskite Ba_2FeWO_6 [120]. Magnetic (Fe) ions occupy alternate octahedra. Possible average magnetic structures obtained by RMC modelling are (b) collinear and (c) non-collinear. (d) The fits to the data are almost identical. Solid curves show the data, collinear and non-collinear fits; dotted curves show the magnetic contributions only; the dashed curve shows the difference of the magnetic contributions $\times$ 10.

10.2. RMCPOW

Inclusion of additional data types, in particular EXAFS data, is also a development goal for RMCPOW. As discussed previously, single-crystal data are more problematic than powder diffraction data, but in general terms one can see that it would be advantageous to be able to combine these as well. A good example that illustrates the need is a study of $Mn_{0.6}Ta_{0.4}O_{1.65}$ [123]. This material shows lattice diffuse scattering due to substitutional disorder of Mn/Ta and O/O vacancies and associated relaxation of the O sublattice. In neutron diffraction there is also magnetic diffuse scattering. X-ray and neutron diffraction data have been combined (figure 14(a), 14(b)), but this information is not sufficient and fails to distinguish sufficiently whether some diffuse scattering peaks are due to atomic or magnetic disorder [46]. Mn or Ta EXAFS data would help. An alternative is the use of polarized neutron diffraction to separate the lattice and magnetic diffuse scattering [124], as shown in figure 14(c) [125]. Figure 14(d) shows a calculated single-crystal pattern based on RMC modelling of powder diffraction data. It can be noted that the pattern is far from isotropic, even though it is based on 'isotropic' data.

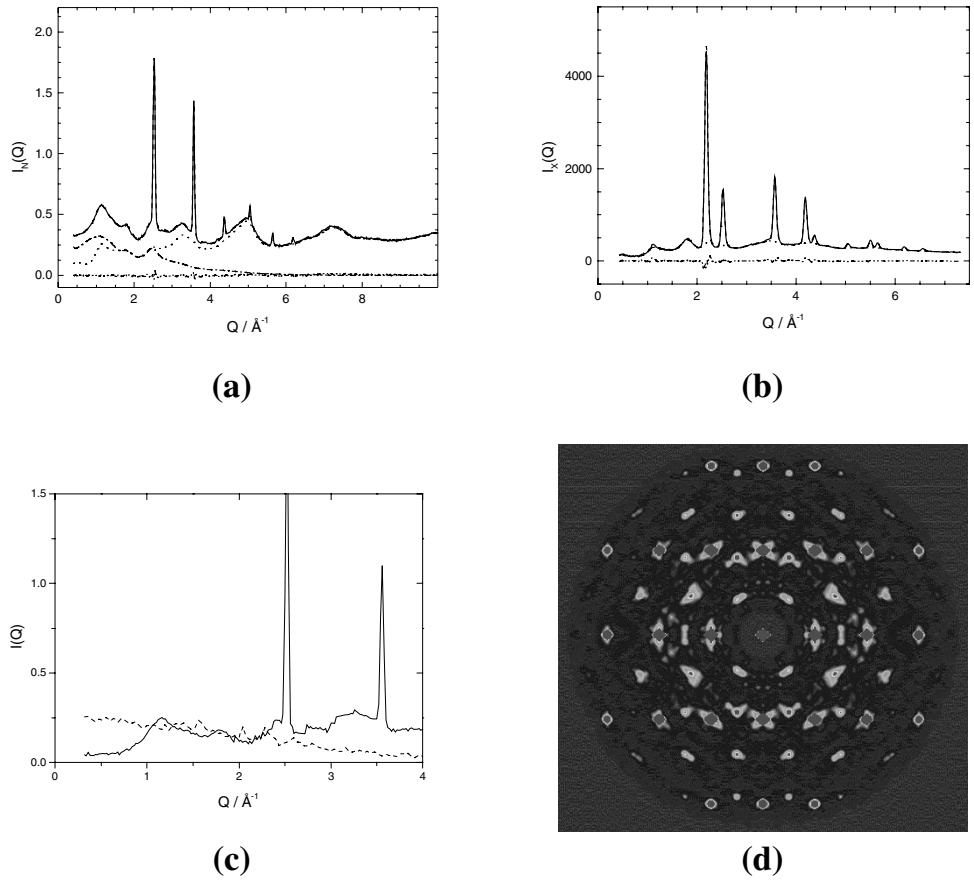

Figure 14. Structure factors for $Mn_{0.6}Ta_{0.4}O_{1.65}$ from (a) neutron and (b) x-ray diffraction; data (solid curves), RMC fit (dashed curve) and the difference (dash–dot–dotted curve); lattice (dotted curve) and magnetic (dash–dotted curve) diffuse scattering [122]. (c) Structure factors for polarized neutron diffraction; nuclear (solid curve) and magnetic (dashed curve) scattering [124]. (d) The single-crystal x-ray diffraction pattern calculated from the RMC model fitted to the powder diffraction data shown.

In fact the positions and directions of the diffuse scattering streaks agree qualitatively with experimental results. The challenge will be to deal with the data corrections, normalization, resolution etc, so that a quantitative comparison can be made.

10.3. New applications

A version of RMC modelling for modelling small-angle scattering data for colloids has been developed [126]. However, this is a special case in that the particles are effectively treated as large 'atoms' and the only variation necessary on the standard RMC procedure is to include the possibility of polydispersity and a scattering form factor (as is already done for x-ray diffraction data). To treat general small-angle scattering data it will be necessary to have 'variable-geometry' particles. One method for doing this is the 'dummy atom' approach of Svergun [127], where a variable-shape large particle (e.g. a biological macromolecule in solution) is represented by a collection of smaller 'dummy atoms'. This has considerable similarity to RMC

modelling, including the use of a type of coordination constraint, in this case called a 'looseness criterion', which controls the compactness of the large particle. Although a simulated annealing algorithm is used to attempt to approach a global minimum, Svergun also notes that the concept of a unique solution is meaningless. There is clear scope for further development of this method to enable application to more general problems than shape reconstruction of single particles. Either the scale could be extended upwards to consider correlations between collections of particles, or downwards towards a more atomistic description.

A program for RMC modelling of reflectivity data has been tested [128]. However, this has the problem that the data has low (real-space) resolution, whereas the RMC model is intrinsically high resolution. The smoothed atomic density may reproduce the data but the individual atomic positions may not make sense unless strong local constraints are applied, and suitable constraints are not necessarily known. However, there may still be possibilities for development in surface studies, for example modelling of off-specular reflectivity data (for which there is currently no general method), particularly for magnetic materials, or surface diffraction data.

A rather different possibility would be in residual stress analysis [129]. In this case the model would be a stress map rather than a set of atom positions. However, the advantages of RMC modelling can be readily translated. As it is an inverse method, it will be easy to include experimental effects (surfaces, absorption, wavelength and intensity variation in the incident beam etc) in the calculation before comparison with the measured data, whereas these are very difficult to deal with by direct methods. Constraints can be applied (e.g. maximum stress gradient) and different data types can be combined. In addition there is a rather natural connection with the widely used method of finite-element modelling, which can be used to calculate the initial stress map.

10.4. Reverse molecular dynamics

As has been discussed earlier, RMC modelling does not produce a unique model. While this is an advantage, nevertheless one should obviously aim to reduce the range of possible models. Diffraction data can be relatively insensitive to some aspects of the structure, but dynamics can be much more sensitive. The next step is therefore to aim to be able to include dynamical information in RMC models, with the long-term goal of producing full dynamical models based on experimental data—'reverse molecular dynamics' (RMD). Development of a prototype algorithm is already under way [130].

11. Conclusions

RMC modelling is now a well established technique and has proved itself able to contribute to our understanding of the structures of a very wide range of materials. It offers unique possibilities for the quantitative combination of a range of different types of complementary experimental data, and for studies of local magnetic order, and there are still many prospects for further development. It would therefore seem that the method is 'here to stay'.

Apart from the detailed aspects that have been discussed in this paper, there are a three general messages that should be taken away. Firstly, accurate and quantitative data are valuable, regardless of whether the data consist of sharp peaks (as in crystalline diffraction) or broad oscillations (as in liquid-state diffraction or EXAFS). Secondly, the act of making 'proper' (e.g. atomistic) structural models leads to considerable insight, often regardless of the exact method used or whether the models agree with the data. Thirdly, there is nothing very clever about RMC modelling—it is simply a combination of the first and second points.

Acknowledgments

I would like to acknowledge the contributions of many people who have worked with me in development of the RMC method—Laszlo Pusztai, Dave Keen, Malcolm Howe, Vicky Nield, Jim Wicks, Per Zetterström and Anders Mellergård. It is also a pleasure to acknowledge the consistent stimulation I have received from the work of Alan Soper. The following are thanked for the provision of data prior to publication: S Kohara, A Mellergård, S Esmaeilzadeh, R Stewart and A K Soper. RMC development is supported by the Swedish Research Council and by the European Commission through the SCANS (Software for Computer Aided Neutron Scattering) network under contract HPRI-CT-1999-50013.

References

[1] McGreevy R L and Pusztai L 1988 *Mol. Simul.* **1** 359
[2] McGreevy R L, Howe M A, Keen D A and Clausen K N 1990 *Neutron Scattering Data Analysis (IOP Conf. Ser. 107)* ed M W Johnson (Bristol: Institute of Physics Publishing) p 165
[3] McGreevy R L and Howe M A 1992 *Annu. Rev. Mater. Sci.* **22** 217
[4] McGreevy R L 1995 *Nucl. Instrum. Methods Phys. Res.* A **354** 1
[5] McGreevy R L 1997 *Computer Modelling in Inorganic Crystallography* ed C R A Catlow (New York: Academic) p 151
[6] Gurman S J and McGreevy R L 1990 *J. Phys.: Condens. Matter* **2** 9463
[7] Keen D A and McGreevy R L 1990 *Nature* **344** 423
[8] McKenzie D R, Davis C A, Cockayne D J H, Muller D A and Cassallo A M 1992 *Nature* **355** 622
[9] McGreevy R L, Howe M A and Wicks J D 1993 *Studsvik Neutron Research Laboratory Internal Report*
[10] Keen D A and McGreevy R L 1991 *J. Phys.: Condens. Matter* **3** 7383
[11] Nield V M, Keen D A and McGreevy R L 1995 *Acta Crystallogr.* A **51** 763
[12] Montfrooij W, McGreevy R L, Hadfield R A and Andersen N-H 1996 *J. Appl. Crystallogr.* **29** 285
[13] Mellergård A and McGreevy R L 1999 *Acta Crystallogr.* A **55** 783
[14] Metropolis N, Rosenbluth A W, Rosenbluth M N, Teller A H and Teller E 1953 *J. Phys. Chem.* **21** 1087
[15] Kaplow R, Rowe T A and Averbach B L 1968 *Phys. Rev.* **168** 1068
[16] Renninger A L, Rechtin M D and Averbach B L 1974 *J. Non-Cryst. Solids* **16** 1
[17] Gerold V and Kern J 1987 *Acta Metall.* **35** 393
[18] Schweika W and Haubold H-G 1988 *Phys. Rev.* B **37** 9240
[19] McGreevy R L and Pusztai L 1990 *Proc. R. Soc.* A **430** 241
[20] Waseda Y, Kang S, Sugiyama K, Kimura M and Saito M 2000 *J. Phys.: Condens. Matter* **12** 195
[21] Bras W, Xu R, Wicks J D, Van der Horst F, Oversluizen M, McGreevy R L and van der Lugt W 1994 *Nucl. Instrum. Methods Phys. Res.* A **346** 394
[22] Wicks J D and McGreevy R L 1997 *Phase Transitions* **61** 195
[23] McLaughlin J C 1999 *J. Mol. Graphics Modell.* **17** 275
[24] Wicks J D, Börjesson L, Bushnell-Wye G, Howells W S and McGreevy R L 1995 *Phys. Rev. Lett.* **74** 726
[25] Pusztai L and McGreevy R L 2001 private communication
[26] Kugler S, Pusztai L, Rosta L, Bellisent R and Chieux P 1993 *Phys. Rev.* B **48** 7685
[27] Keen D A 1997 *Phase Transitions* **61** 109
[28] Kohara S 2001 private communication
[29] Pusztai L and McGreevy R L 1999 *J. Neutron Res.* **8** 17
[30] McGreevy R L and Pusztai L 1998 *Electrochim. Acta* **43** 1349
[31] Carlsson P, Swenson J, Börjesson L, Torell L M, McGreevy R L and Howells W S 1998 *J. Chem. Phys.* **109** 8719
[32] Karlsson L and McGreevy R L 1995 *Solid State Ion.* **76** 301
[33] Evans R A 1990 *Mol Simul.* **4** 409
[34] Soper A K 2001 *Mol. Phys.* **99** 1503
[35] Howe M A and McGreevy R L 1991 *Phys. Chem. Liq.* **24** 1
[36] Colognesi D, de Santis A and Rocca D 1996 *Mol. Phys.* **88** 465
[37] Howe M A 1990 *Mol. Phys.* **69** 161
[38] Stolz M, Winter R, Howells W S, McGreevy R L and Egelstaff P A 1994 *J. Phys.: Condens. Matter* **6** 3619
[39] Scheidler M, North A N and Dore J C 1993 *Mol. Simul.* **11** 345

[40] Howe M A, McGreevy R L, Pusztai L and Borzsak I 1993 *Phys. Chem. Liq.* **25** 204
[41] Soper A K 1990 *Neutron Scattering Data Analysis (IOP Conf. Ser. 107)* ed M W Johnson (Bristol: Institute of Physics Publishing) p 192
[42] Nield V M, Keen D A, Hayes W and McGreevy R L 1992 *J. Phys.: Condens. Matter* **4** 6703
[43] Mellergård A 2001 private communication
[44] Belushkin A V, Kozlenko D P, McGreevy R L, Savenko B N and Zetterström P 1999 *Physica* B **269** 297
[45] McGreevy R L and Mellergård A 1999 *AIP Conf. Ser.* **479** 19
[46] Mellergård A and McGreevy R L 2000 *Chem. Phys.* **261** 267
[47] Andreev Y G and Bruce P G 1998 *Mater. Sci. Forum* **278–281** 14
[48] Tucker M G, Squires M P, Dove M T and Keen D A 2001 *J. Phys.: Condens. Matter* **13** 403
[49] Tucker M G, Dove M T and Keen D A 2001 *J. Appl. Crystallogr.* submitted
[50] Proffen T and Neder R B 1997 *J. Appl. Crystallogr.* **30** 171
[51] Proffen T 1997 *Acta Crystallogr.* **53** 202
[52] Proffen T 1997 *Z. Kristallogr.* **212** 764
[53] Toth G and Baranyai A 1997 *J. Chem. Phys.* **107** 7402
[54] Toth G and Baranyai A 1999 *Mol. Phys.* **97** 339
[55] Toth G and Baranyai A 2000 *J. Mol. Liq.* **85** 3
[56] da Silva F L B 1998 *J. Chem Phys.* **109** 2624
[57] Toth G, Pusztai L and Baranyai A 1999 *J. Chem. Phys.* **111** 5620
[58] da Silva F L B, Svensson B, Åkesson T and Jonsson B 1999 *J. Chem. Phys.* **111** 5622
[59] da Silva F L B, Olivares-Rivas W, Degreve L and Åkesson T 2001 *J. Chem. Phys.* **114** 907
[60] Adams S and Swenson J 2000 *Phys. Rev. Lett.* **84** 4144
[61] Adams S and Swenson J 2001 *Phys. Rev.* B **63** 054201
[62] Mellergård A 2001 private communication
[63] Gehlen P C and Cohen J B 1965 *Phys. Rev.* A **139** 844
[64] Kirkpatrick S, Gelatt C D Jr and Vecci M P 1983 *Science* **220** 671
[65] Schommers W 1983 *Phys. Rev.* A **28** 3599
[66] Levesque D, Weiss J J and Reatto L 1985 *Phys. Rev. Lett.* **54** 451
[67] Lyubartsev A B 1995 *Phys. Rev.* E **52** 3730
[68] Soper A K 1996 *Chem. Phys.* **202** 295
[69] Neuefeind J, Fischer H E and Schröder W 2000 *J. Phys.: Condens. Matter* **12** 8765
[70] Toth G 2000 *J. Mol. Liq.* **85** 3
[71] Landron C, Soper A K, Jenkins T, Greaves G N, Hennet L and Coutures J-P 2001 *J. Non-Cryst. Solids* **293–295** 453
[72] Car R and Parrinello M 1985 *Phys. Rev. Lett.* **55** 2471
[73] Foley M, Smargiassi E and Madden P A 1994 *J. Phys.: Condens. Matter* **6** 5231
[74] Delaye J-M, Ghaleb D, Cormier L and Calas G 2001 *J. Non-Cryst. Solids***293–295** 290
[75] Winter R and Hensel F 1989 *Phys. Chem. Liq.* **20** 1
[76] Nield V M, Howe M A and McGreevy R L 1991 *J. Phys.: Condens. Matter* **3** 7519
[77] Arai T and McGreevy R L 1999 *Phys. Chem. Liq.* **37** 455
[78] Franz J R 1986 *Phys. Rev. Lett.* **57** 889
[79] Arai T and McGreevy R L 1998 *J. Phys.: Condens. Matter* **10** 9221
[80] Howe M A and McGreevy R L 1991 *J. Phys.: Condens. Matter* **3** 577
[81] Reijers H T J, Saboungi M-L, Price D L, Richardson J W Jr, Volin K J and van der Lugt W 1989 *Phys. Rev.* B **40** 6018
[82] van der Aart S A 1999 *Phys. Scr.* **59** 157
[83] Hafner J, Seifert-Lorenz K and Genser O 1999 *J. Non-Cryst. Solids* **250–252** 225
[84] de Wijs G A, Pastore G, Selloni A and van der Lugt W 1994 *Europhys. Lett.* **77** 667
[85] de Wijs G A, Pastore G, Selloni A and van der Lugt W 1995 *J. Chem. Phys.* **103** 5031
[86] Genser O and Hafner J 1999 *J. Non-Cryst. Solids* **250–252** 236
[87] Kirchoff F, Holender J M and Gillan M J 1996 *Phys. Rev.* B **54** 190
[88] Swenson J, McGreevy R L, Börjesson L and Wicks J D 1998 *Solid State Ion.* **105** 55
[89] Börjesson L, Torell L M, Dahlborg U and Howells W S 1989 *Phys. Rev.* B **39** 3404
[90] Swenson J and Börjesson L 1996 *Phys. Rev. Lett.* **77** 3569
[91] Varsamis C P, Kamitsos E I and Chryssikos G D 1999 *Phys. Rev.* B **60** 3885
[92] Nield V M 1995 *Nucl. Instrum. Methods Phys. Res.* A **354** 30
[93] Nield V M and Whitworth R W 1995 *J. Phys.: Condens. Matter* **7** 8259
[94] Beverley M N and Nield V M 1997 *J. Phys. Chem.* B **101** 6188

[95] Beverley M N and Nield V M 1997 *J. Phys.: Condens. Matter* **9** 5145
[96] Proffen T 1997 *Physica* B **241** 281
[97] Proffen T and Welberry T R 1998 *J. Appl. Crystallogr.* **31** 318
[98] Proffen T and Welberry T R 1998 *Phase Transitions* **67** 373
[99] Keen D A, McGreevy R L and Hayes W 1990 *J. Phys.: Condens. Matter* **2** 2773
[100] Keen D A, Hayes W, McGreevy R L and Clausen K N 1990 *Phil. Mag. Lett.* **61** 349
[101] Nield V M, Keen D A, Hayes W and McGreevy R L 1993 *Solid State Ion.* **66** 24
[102] Nield V M, McGreevy R L, Keen D A and Hayes W 1994 *Physica* B **202** 159
[103] Keen D A and Hull S 1998. *J. Phys.: Condens. Matter* **10** 8217
[104] Chahid A and McGreevy R L 1998 *J. Phys.: Condens. Matter* **10** 2597
[105] Tucker M G, Dove M T and Keen D A 2000 *J. Phys.: Condens. Matter* **12** 1723
[106] Belushkin A V, Kozlenko D P, McGreevy R L, Savenko B N and Zetterström P 1999 *Physica* B **269** 297
[107] Kozlenko D P, Belushkin A V, Knorr K, McGreevy R L, Savenko B N and Zetterström P 2001 *Physica* B **299** 46
[108] Andersen N-H, Bandaranayake P W S K, Careem M A, Dissanayake M A K L, Wijayasekera C N, Kaber Lundén R A, Mellander B-E, Nilsson L and Thomas J O 1992 *Solid State Ion.* **57** 203
[109] Secco E A 1993 *Solid State Ion.* **60** 233
[110] Belushkin A V, Carlile C J and Shuvalov L A 1992 *J. Phys.: Condens. Matter* **4** 389
[111] Zetterström P, Belushkin A V, McGreevy R L and Shuvalov L A 1999 *Solid State Ion.* **116** 321
[112] Hannon A C, Wright A C and Sinclair R N 1991 *Mater. Sci. Eng.* A **134** 883
[113] Keen D A, McGreevy R L, Bewley R I and Cywinski R 1995 *Nucl. Instrum. Methods Phys. Res.* A **354** 48
[114] Keen D A, Bewley R I, Cywinski R and McGreevy R L 1996 *Phys. Rev.* B **54** 1036
[115] Karlsson L, Wannberg A, McGreevy R L and Keen D A 2000 *Phys. Rev.* B **61** 487
[116] Karlsson L, McGreevy R L and Wicks J D 1999 *J. Phys.: Condens. Matter* **11** 9249
[117] Mellergård A and McGreevy R L 1998 *J. Phys.: Condens. Matter* **10** 9401
[118] Mellergård A, McGreevy R L and Eriksson S G 2000 *J. Phys.: Condens. Matter* **12** 497
[119] Mompean F J, Mellergård A, Garcia-Hernandez M, Sanchez-Soria D, de Andres A, McGreevy R L and Martinez J L 2001 *J. Alloys Compounds* **323–324** 404
[120] Garcia-Hernandez M, Mellergård A, Mompean F J, Sanchez D, de Andres A, McGreevy R L and Martinez J L 2001 *Phys. Rev. Lett.* submitted
[121] Azad A K, Eriksson S G, Eriksen J, Ivanov S A, Mellergård A and Rundlöf H 2001 private communication
[122] Winterer M, Delaplane R G and McGreevy R L 2001 *J. Appl. Crystallogr.* submitted
[123] Esmaeilzadeh S 2000 Crystal chemistry of manganese tantalum oxides *Doctoral Thesis* Stockholm University, Sweden
[124] Cywinski R, Kilcoyne S H and Stewart J R 1999 *Physica* B **267–268** 106
[125] Mellergård A, Esmaeilzadeh S and Stewart J R 2001 private communication
[126] Toth G and Pusztai L 1992 *J. Chem. Phys.* **96** 7150
[127] Svergun D I 1999 *Biophys. J.* **76** 2879
[128] Rycroft S 2000 private communication
[129] McGreevy R L 2001 private communication
[130] Zetterström P, McGreevy R L and Ebbsjö I 2001 private communication